The Influence of Design Variations on CTR Blanket Neutronic Performance Using Variational Techniques

E. Cheng and R.W. Conn

June 1976

UWFDM-169

Accepted for publication in *Nuclear Science and Engineering.*

FUSION TECHNOLOGY INSTITUTE

UNIVERSITY OF WISCONSIN

MADISON WISCONSIN

The Influence of Design Variations on CTR Blanket Neutronic Performance Using Variational Techniques

E. Cheng and R.W. Conn

Fusion Technology Institute
University of Wisconsin
1500 Engineering Drive
Madison, WI 53706

http://fti.neep.wisc.edu

June 1976

UWFDM-169

Accepted for publication in *Nuclear Science and Engineering.*

The Influence of Design Variations on CTR Blanket Neutronic Performance Using Variational Techniques

by

Edward T. Cheng
and
Robert W. Conn

Fusion Technology Program
Nuclear Engineering Department
The University of Wisconsin
Madison, Wisconsin 53706

June 1976

Accepted for Publication in Nuclear Science and Engineering

Abstract

The influence of design variations, such as the percentage of structural material in a tritium breeding zone or the enrichment of lithium in ^{6}Li, on important CTR parameters like the tritium breeding ratio and the total nuclear energy produced has been studied using variational techniques for two different but general blanket designs. The first design uses liquid lithium as both the coolant and breeding material while the second uses a helium coolant and a solid lithium bearing compound as the tritium breeder. A variational technique based upon variational interpolation is the primary computational tool and it is shown that for linear perturbations in the transport operator and for a fixed source, only forward flux calculations are required to implement the variational interpolation approach. No adjoint functions are required while any number of response functionals can be investigated. For both blanket designs the influence of the choice of structural material such as stainless steel, molybdenum, niobium, vanadium, and aluminum structures has been studied. The role of beryllium as a neutron multiplier with a solid breeder blanket is also studied and an optimum beryllium thickness is found which maximizes the breeding ratio. The influence of using graphite or the structural material as a neutron reflector and the effect of lithium burnup are also studied. It is found that for a given percentage of structural material in the tritium breeding zones, vanadium structured systems achieve the highest breeding ratios while molybdenum structured systems produce the highest value of total nuclear heating. The effects of lithium burnup are small.

I. Introduction

In the study of fusion reactor blankets, the most important quantities are linear functionals of the neutron flux and can be written as a scalar product, $(S^{\dagger},\phi)$. In general, estimates of these linear functionals are possible using variational methods together with particular solutions to the Boltzmann transport equation,

$$L(\alpha)\phi_{\alpha} = S(\alpha); \tag{1}$$

and the adjoint equation,

$$L^{\dagger}(\alpha)\phi^{\dagger}_{\alpha} = S^{\dagger}(\alpha). \tag{2}$$

Here, α is a characteristic parameter in the system and $S^{\dagger}$ is the response function for the estimate.

Variational methods based on the Roussopoulos and Schwinger functionals, as well as the variational synthesis method, are well known and have been widely investigated.[1-5] In these approaches, the estimate can be approximated by the following functionals:

Roussopoulos (bilinear) functional:

$$I_R(\phi^{\dagger}_1,\phi_1;\alpha) = (S^{\dagger}(\alpha),\phi_1) + (\phi^{\dagger}_1, S(\alpha) - L(\alpha)\phi_1) \tag{3}$$

Schwinger (fractional) functional:

$$I_s(\phi^{\dagger}_1,\phi_1;\alpha) = \frac{(\phi^{\dagger}_1,S(\alpha))\ (S^{\dagger}(\alpha),\phi_1)}{(\phi^{\dagger}_1,L(\alpha)\phi_1)} \tag{4}$$

Variational synthesis functional:[a]

$$I_{vs}(\alpha) = (S^{\dagger}(\alpha),\phi_1) + \frac{(\phi_2^{\dagger} - \phi_1^{\dagger},S(\alpha) - L(\alpha)\phi_1)\ (S^{\dagger}(\alpha),\phi_2 - \phi_1)}{(\phi_2^{\dagger} - \phi_1^{\dagger},L(\alpha)\ (\phi_2 - \phi_1))} \tag{5}$$

where ϕ_1 and ϕ_2 satisfy $L(\alpha_1)\phi_1 = S(\alpha_1)$ and $L(\alpha_2)\phi_2 = S(\alpha_2)$, respectively, and $\phi_1^{\dagger}$ and $\phi_2^{\dagger}$ satisfy $L^{\dagger}(\alpha_1)\phi_1^{\dagger} = S^{\dagger}(\alpha_1)$ and $L^{\dagger}(\alpha_2)\ \phi_2^{\dagger} = S^{\dagger}(\alpha_2)$, respectively.

A multipoint variational interpolation (VI) method based on variational principles has recently been presented by the authors[6]. The basic idea is to use a variational principle together with either a forward solution or adjoint solution at each of several reference points to estimate the value of a **linear functional** at points other than the reference ones. The simplest example of the method is a two-point interpolation using the functional

$$I_{VI}(\phi_2^{\dagger},\phi_1;\alpha) = (S^{\dagger}(\alpha),\phi_1) + (\phi_2^{\dagger},S(\alpha) - L(\alpha)\phi_1) \tag{6}$$

where α represents an interpolation parameter. This functional is exact at $\alpha = \alpha_1$ or $\alpha = \alpha_2$ and can be used to estimate values of the scalar product, $(S^{\dagger}(\alpha),\phi)$, at other values of the parameter α. Functionals have been developed for $(S^{\dagger}(\alpha),\phi)$ which are exact at N arbitrary points, $\{\alpha_i\}$,i = 1,2,...,N, using only a single reference forward solution or adjoint at each of the reference points. This removes the normal requirement to compute a forward solution and a corresponding adjoint at each reference point, α_i. A more detailed description of the theoretical development can be found in reference 6.

---

[a] The derivation of this functional is same as presented in reference 6.

Let $\phi_t(\alpha) = \phi_1 + a(\alpha)\ (\phi_2 - \phi_1)$

$\phi_t^{\dagger}(\alpha) = \phi_1^{\dagger} + a^{\dagger}(\alpha)\ (\phi_2 - \phi_1)$

and use the standard Rayleigh-Ritz procedure to determine the coefficients $a(\alpha)$ and $a^{\dagger}(\alpha)$ for any α.

Here we present computational results on the application of variational methods to two types of fusion reactor blanket designs, liquid lithium cooled blankets and solid breeder, helium cooled blankets. The systems developed for UWMAK-I[7] and UWMAK-II[8] conceptual tokamak reactors will be used as standards. In Section II, a simplification of the variational approach for fixed source problems (the most common kind) is shown to produce considerable computational savings. In particular, it eliminates the need for computing adjoint fluxes in fixed source perturbation theory calculations. Comparison of standard variational procedure and the variational interpolation method is also given in this section. The results of computations using the variational interpolation method to study the design variations in the UWMAK-I and UWMAK-II CTR blanket system are discussed in Section III. Here we study the effect of using different structural materials and various enrichments of lithium in ^{6}Li. In the last section, we present a variational analysis of the impact of lithium burnup on the tritium breeding ratio.

II. Theory and Computational Error Analysis

A. Simplification for Fixed Source Problems

The general theory of variational interpolation has been given elsewhere[6]. However, an important simplification is possible when the source is fixed as is generally the case in fusion reactor blanket neutronic calculations. This is because one is typically interested in many reaction rates simultaneously and these can each be calculated as simple scalar products once a forward solution, i.e., the neutron flux, is known.

The method of variational interpolation can be formulated to require only forward fluxes; no adjoint calculations are required to obtain information concerning linear functionals provided that the perturbation is linear. This can be demonstrated briefly using a two-point interpolation. Suppose

ϕ_1 and ϕ_2 are solutions to the transport equation, Eqn. (1), corresponding to systems with parameters $\alpha = \alpha_1$ and $\alpha = \alpha_2$. The value of the variational functional to approximate the linear functional, $(S^\dagger(\alpha),\phi)$, for any α is given by Eqn. (6). It has been shown that this estimate is exact at $\alpha = \alpha_1$ or α_2. Upon rewriting Eqn. (6), the second term on the right hand side becomes $-(\phi_2^\dagger,\delta L(\alpha)\phi_1)$, where $L(\alpha_1)\phi_1 = S$ is used and the perturbation operator $\delta L(\alpha)$ is defined by

$$\delta L(\alpha) = L(\alpha) - L(\alpha_1). \tag{7}$$

If the perturbation can be written as the product of any function $f(\alpha)$ and a bounded operator H, i.e.,

$$\delta L(\alpha) = f(\alpha)H \tag{8}$$

where $H = [L(\alpha_2) - L(\alpha_1)]/f(\alpha_2)$, and $f(\alpha_1) = 0$ because of $\delta L(\alpha_1) = 0$. Eqn. (6) becomes

$$I_{VI}(\phi_2^\dagger,\phi_1;\alpha) = (S^\dagger(\alpha),\phi_1) - \frac{f(\alpha)}{\alpha_2 - \alpha_1}(\phi_2^\dagger,H\phi_1). \tag{9}$$

When $\alpha = \alpha_2$, $I_{VI}(\phi_2^\dagger,\phi_1;\alpha_2) = (\phi_2^\dagger,S)$, which is exact. Thus we have

$$f(\alpha_2)\,(\phi_2^\dagger,H\phi_1) = (S^\dagger(\alpha_2),\phi_1) - (S^\dagger(\alpha_2),\phi_2) \tag{10}$$

where the adjoint relation $(\phi_2^\dagger,S) = (S^\dagger(\alpha_2),\phi_2)$ is used. Hence for any α, the functional I_{VI} can be written in terms of ϕ_1 and ϕ_2 as

$$I_{VI}(\phi_2,\phi_1;\alpha) = (S^\dagger(\alpha),\phi_1) - \frac{f(\alpha)}{f(\alpha_2)}\left\{(S^\dagger(\alpha_2),\phi_1) - (S^\dagger(\alpha_2),\phi_2)\right\}. \tag{11}$$

Note here that the functional given by Eqn. (11) is linear in α due to the basic form of the Roussopoulos functional. The fractional form (based on the Schwinger functional) may also be written in terms of ϕ_1 and ϕ_2 as

$$I_s(\phi_2,\phi_1;\alpha) = \frac{(S^\dagger(\alpha),\phi_1)\;(S^\dagger(\alpha_2),\phi_2)}{(S^\dagger(\alpha_2),\phi_2) + \frac{f(\alpha)}{f(\alpha_2)}\{(S^\dagger(\alpha_2),\phi_1) - (S^\dagger(\alpha_2),\phi_2)\}}. \tag{12}$$

Since Eqns. (11) and (12) are written only in terms of the forward fluxes (ϕ_1 and ϕ_2), no adjoint calculation is required. Two such calculations are all that is required to interpolate in α on the functional $(S^\dagger(\alpha),\phi)$ for any $S^\dagger(\alpha)$. Thus two calculations suffice to estimate an arbitrary number of linear functionals. This is in contrast to the normal formulation where an adjoint calculation is required for each $S^\dagger(\alpha)$ of interest.

The theory of variational interpolation is, in general, derived for any possible perturbation in the system and the simplification for fixed source and linearly perturbed problems can be carried through for several perturbation parameters, α_i. In addition, it is clear that one can completely reverse the derivation and determine the functional $(\phi^\dagger,S) = (S^\dagger,\phi)$ using only two adjoint functions, $\phi_1^\dagger$ and $\phi_2^\dagger$, for problems where $S^\dagger$ is fixed and $L^\dagger(\alpha)$ depends linearly on α. Here, no forward calculations would be required. The computational error analysis for a problem with two parameters varying simultaneously (e.g., the percent structure and the enrichment of lithium in ^{6}Li) will be discussed in the following subsection.

B. Computational Error Analysis

A comparison of computational results for the tritium breeding ratio using various variational functionals will be used to indicate the accuracy of the methods. The perturbation parameter is the percent change of structural material in the breeding zones of the blanket. The specific blanket design used as a model is that from the conceptual reactor design, UWMAK-I[7], which consists of a 4 mm first wall, a 51 cm homogenized breeding zone of liquid lithium and structure, a 15 cm reflector of the basic structural material, and a 5 cm homogenized zone of liquid lithium and structure. The structure is stainless steel in the standard design. The schematic of the UWMAK-I blanket is given in Figure 1. The one-dimensional transport code, ANISN[9], is used for the forward flux and adjoint function calculations in this and the following sections. The calculations are done in slab geometry. The

variational code, SWANLAKE[10], is used to compute scalar products and bilinear forms.

We define T_6 as the tritium production per neutron from $^6Li(n,\alpha)$ reaction and T_7 as the tritium production per neutron from $^7Li(n,n\alpha)$ reaction and the sum over T_6 and T_7 is the desired tritium breeding ratio. We have chosen 5% and 25% structure in the breeding zones as reference points (α_1 corresponds to the 5% system and α_2 to the 25% system). At 5% structure, T_6 and T_7 are 0.861 and 0.579 respectively. The tritium breeding ratio is, therefore, 1.440 which is more than required for a D-T fusion reactor. At 25% structure, T_6 and T_7 are 0.836 and 0.268, respectively, and the tritium breeding ratio is 1.104. Thus as the percent structure is increased from 5% to 25%, T_6 is only slightly decreased (by ~ 3%) while T_7 decreases much more (by ~ 54%). The tritium breeding ratio is lowered by ~ 23%.

The Schwinger and other variational functionals have been used to estimate T_6 and T_7 as the percentage of structural material in the breeding zone is varied away from the two reference points. The results are shown in Fig. 2. We note that using Eqn. (4) with α_1 at 5%, as the reference, the maximum error in T_7 at $\alpha = \alpha_2$ is about 5%. However, the error in both T_6 and T_7 is steadily increasing as α increases. By contrast, the VI method is exact at α_1 and α_2 and from the characteristic of cancellation of error[6], the error at values of α between α_1 and α_2 is less than 2% for T_7 and less than 1% for T_6. Specific values for T_6 and T_7 at various values of percentage structure using three methods, the Schwinger functional, variational interpolation in the fractional form, and the synthesis method, are tabulated in Table 1. Note that when the synthesis functional, Eqn. (5), is applied (ϕ_1 and $\phi_1^\dagger$ at 5%, ϕ_2 and $\phi_2^\dagger$ at 25% structure), the results are very accurate.

Note that to apply either the ordinary Schwinger functional or the synthesis method requires both forward and adjoint trial functions. Only one forward flux at each reference point is used in the application of variational interpolation since the change of percent structure can be written as a linear function of a parameter.

We have used this same problem also to test the accuracy of the VI method for estimating the tritium breeding ratio and total nuclear heating when there are two perturbation parameters, the percent structure in the breeding zones and the ^{6}Li enrichment. We find comparably accurate results as summarized in Table 2.

One can conclude that estimating the tritium breeding ratio and total nuclear heating for the UWMAK-I type blankets using the simplified VI technique will be adequate, particularly for initial design analyses and survey calculations.

III. Applications

In this section, two conceptual blanket designs will be examined using variational methods, particularly the VI technique, and we will study the effect of changes in important design parameters on the tritium breeding ratio and total nuclear heating. The systems investigated here are the blanket designs recently developed at the University of Wisconsin, UWMAK-I and UWMAK-II.

A. UWMAK-I Blanket[7]

The standard UWMAK-I blanket design has been discussed and is shown in Fig. 1. In addition to design variations already discussed, one is interested in the effect of choosing other structural materials. In particular, materials like niobium, molybdenum, vanadium and aluminum will be considered. Reference points are taken at 5% and 25% structure in the breeding zones and lithium with 7.42% ^{6}Li (natural) and 30% ^{6}Li in the lithium. A particular blanket in which the 15 cm stainless steel reflector is replaced by a 30 cm graphite reflector is discussed at the end of this subsection.

A-1. Reference System Results and Interpolations

Tables 3-7 show the reference values for T_6, T_7, the tritium breeding ratio and total nuclear heating in blankets with 316 stainless steel, niobium, vanadium, molybdenum or aluminum as the structural material. Some important results may be summarized as follows. When the percent structure in the breeding zones increases, T_7 decreases while T_6 decreases slightly in a natural lithium blanket. For the blanket structural materials considered here, the only exception to the above effect is vanadium. T_6 increases slightly for a vanadium blanket because the parasitic absorption for neutrons interacting with vanadium is small compared with that in the other materials. For all systems, the tritium breeding ratio is in excess of 1.2 when the percent structure is doubled from the standard design (5%). Niobium is the only exception due to its relatively higher capture cross section.

For blankets with lithium enriched to 30% ^{6}Li, T_6 increase slightly except the aluminum structured blanket. For an aluminum structured system, the neutron spectrum is not as soft, hence T_6 is still decreasing as the lithium concentration decreases. In a stainless steel blanket, the overall tritium breeding ratio decreases as the percent structure increases. However, as shown in Fig. 3, enriching the lithium in ^{6}Li can lead to more optimal breeding ratios once the amount of structure increases beyond about 15%.

The tritium breeding ratio as a function of ^{6}Li enrichment is essentially determined by the variation of T_7 for a blanket with moderate ^{6}Li concentration. When the ^{6}Li enrichment increases, there is a simultaneous decrease in the ^{7}Li concentration and thus in T_7. The spatial distributions of T_6 and T_7 in the breeding zones for the stainless steel blankets with various ^{6}Li enrichments

(7.42%, 20% and 30%) are depicted in Figure 4. The values for the tritium breeding as a function of ^{6}Li enrichment are shown in Figure 5. From this figure, it is clear that the maximum tritium breeding ratio in a stainless steel blanket occurs at a value of 10-25% ^{6}Li enrichment. However, the increase of the tritium breeding ratio over that from a typical natural lithium cooled blanket varies only from 1-7% depending on the value of percent structure in the blanket (from 5% to 25%). For a standard (5% structure) niobium or molybdenum blanket, this increase of the tritium breeding ratio is about 10%. Thus one may conclude that natural lithium yields a tritium breeding ratio close to the maximum for most practical blanket designs.

Values of total nuclear heating as a function of the percent structure and of the ^{6}Li enrichment in the breeding zones are shown in Figures 6 and 7, respectively. From these figures, one can see that the energy released from neutron interactions with ^{6}Li and ^{7}Li show the same trends as that for T_6 and T_7. However, it has been found that the change in the total nuclear heating is not very sensitive over the parameter range of design interest. The reason is that the increased exothermic reactions in the structure offset losses of energy due to decreased neutron capture in ^{6}Li.

Fig. 8 shows equi-tritium breeding ratio contours for variations in the two perturbation parameters. Several exact values are given on this figure. The corresponding total nuclear heating is indicated in parenthesis. Note that the total nuclear heating in a natural lithium blanket increases by about 3% while the tritium breeding ratio decreases by 24% as the percent structure varies from 5% to 25%.

A-2. Niobium Structure and Reflector

Niobium is a refractory metal which has high neutron parasitic absorption when compared with the other structural materials. For a standard blanket of natural lithium and niobium, the tritium breeding ratio is about 1.30 and drops below 1.00 for blankets with more than 15% structure, as shown on Figure 9(A).

However, when the liquid lithium is enriched in ^{6}Li to more than 20%, the tritium breeding ratio is larger than that for a stainless steel blanket. This can be seen on Figure 10(A). The reason is that the increase of the ^{6}Li concentration reduces the neutron parasitic capture in the niobium structure relative to capure in ^{6}Li. As far as the total nuclear heating is concerned, Figures 9(B) and 10(B) show that this value is larger in a niobium blanket than in all other blankets except molybdenum. Note here that for a natural lithium cooled system, the total nuclear heating in a standard (5% structure) niobium blanket is approximately 5% larger than in a standard stainless steel blanket and about 14% larger than in a standard aluminum blanket. The equi-breeding ratio contours for variations in the range of interest are presented on Figure 11 and the total nuclear heating is given in parenthesis.

A-3. Molybdenum Structure and Reflector

As shown on Figures 9(A) and 10(A), a natural lithium blanket with molybdenum as the structure exhibits a tritium breeding potential that is between blankets with stainless steel and niobium structure. As the ^{6}Li concentration is increased, the tritium breeding ratio of a standard molybdenum blanket reaches a plateau value of about 1.54 at about 15% ^{6}Li and remains at that level out to as much as 40% ^{6}Li in the lithium. Also, a molybdenum blanket produces the largest total nuclear heating of any structural material used at equal volume percentage. An equi-breeding ratio contour plot for a molybdenum structured blanket is given in Fig. 12.

A-4. Vanadium Structure and Reflector

A vanadium structured blanket shows the best tritium breeding ratio, about 1.6, for the standard (5% structure) design. However, the total nuclear heating in this blanket is 15.6 MeV per D-T neutron which is very close to that in a standard stainless steel blanket. The trends of the tritium breeding and the total energy production are similar to a stainless steel blanket. Equi-breeding ratio contours are shown on Fig. 13.

A-5. Aluminum Structure and Reflector

Aluminum is an element which has very low neutron parasitic absorption, but the neutron multiplication cross section, (n,2n), for 14 MeV neutrons on aluminum is about one-fifth that of vanadium or iron, and is about one-tenth that of niobium or molybdenum. The Al (n,2n) threshold energy is very high (~ 13.5 MeV) and the high energy neutron slowing down power is the poorest of the materials being discussed. This leads to a hard neutron spectrum in the breeding zones. From Tables 3 to 7, we see that T_7 for blankets with aluminum structure is the largest while T_6 is still better than in niobium structured blankets when natural lithium is used. The overall tritium breeding ratio in an aluminum structured blanket is, in general, very close to that in a blanket with stainless steel structure. The total nuclear heating in an aluminum structured blanket is the lowest of all the blankets studied. The trends followed by the tritium breeding ratio and total nuclear heating are easily compared in Figures 9 and 10. The equi-breeding ratio contours are depicted on Fig. 14 and can be seen to be very similar to those in a stainless steel structured blanket (see Fig. 8).

A-6. Stainless Steel Structure and Graphite Reflector

If the stainless steel reflector shown on Fig. 1 is replaced by 30 cm of graphite in a standard stainless steel structured blanket, T_6 is increased because of additional reflected neutrons.

Compared with Tables 3 and 8 for a standard design (5% structure) with natural lithium as coolant, the tritium breeding ratio and total nuclear heating for this modified blanket are higher (~ 6% and 3% respectively) than the original UWMAK-I design. For a blanket with a moderate ^{6}Li enrichment (~ 30%), T_6 is increased and the overall effect is that the tritium breeding ratio is slightly increased as compared to the blanket with stainless steel reflector. The equi-breeding ratio contour plot is given in Fig. 15.

B. UWMAK-II Blanket[8,11]

The UWMAK-II blanket design is aimed at minimizing both the tritium and the lithium inventory in the blanket. The design as shown in Fig. 16 consists of a 1 cm first wall (net), 3 cm and 10 cm breeding zones divided by a 18 cm beryllium neutron multiplier zone, and a 38 cm graphite reflector. The density factors in the breeding zones, beryllium multiplier zone and graphite reflector zone are 0.5, 0.5 and 0.8, respectively. This is to allow for helium coolant passages. The structure is taken as 10% of the volume everywhere. Lithium aluminate, $Li_2 Al_2 O_4$, with 90% ^6Li in the total lithium is used as breeding material. Several important variations on the blanket were investigated and the results are summarized as follows.

B-1. First Wall Thickness

In general, the neutron flux distribution and the number of Be(n,2n) reactions depend upon the first wall thickness. It is found that the number of Be(n,2n) reactions increases by ~ 18%, the tritium breeding ratio increases by ~ 4.6% and the total nuclear heating increases by ~ 2.2% when the first wall thickness is decreased to 5 mm (net). Conversely, increasing the first wall thickness causes a decrease in the tritium breeding ratio because of spectral softening and parasitic absorption. A summary of these results is given on Fig. 17.

B-2. Percent Structure Variation

In the UWMAK-II blanket, the net volume percent of structure in the breeding

and neutron multiplication zones is effectively 5%. Tables 9-11 summarize the effect of changing the amount of structure in the breeding and multiplying zones on the tritium breeding ratio, the neutron balance and the total nuclear heating.

B-3. Beryllium Zone Thickness

As the thickness of the beryllium zone is increased, Be(n,2n) reactions increase until a saturation level is reached. However, parasitic absorption in the additional stainless steel structure in that zone also increases and eventually overtakes the positive influence of Be(n,2n) reactions. As such, there is an optimum beryllium thickness at which the tritium breeding ratio is a maximum. Three point variational interpolation has been used to determine this maximum with reference systems chosen with 9cm, 27 cm and 36 cm thick beryllium zones. Results are also summarized on Tables 9-11. The spatial distribution of the tritium breeding ratio (primarily T_6) and Be(n,2n) reactions for blankets with beryllium zones of 9 cm, 18 cm and 27 cm are shown in Fig. 18 while the tritium breeding ratio as a function of beryllium zone thickness is depicted on Fig. 19 (from three-point interpolation). The conclusions are that T_6 in the first breeding zone (zone 4) is proportional to the Be(n,2n) reactions and eventually saturates as beryllium zone becomes thicker, that T_6 in the second breeding zone (zone 6) decreases as the beryllium zone thickness increases, and that the optimum beryllium zone thickness is about 20 cm. At this thickness, the breeding ratio reaches its maximum value of 1.2. All these results are summarized in the equi-breeding ratio contour plot shown on Fig. 20.

C. Lithium Burnup

The tritium breeding element, lithium, is burned up while producing tritium. The burnup rates for the isotopes, ^6Li and ^7Li in UWMAK-I and UWMAK-II blankets for one year of continuous operation with $1MW/m^2$ neutron wall loading, are tabulated in Table 12. The change in the macroscopic cross section for tritium production due

to burnup is $\Sigma = \Sigma_o + \delta\Sigma$, where $\delta\Sigma = (\delta N_7)\sigma_{T_7} + (\delta N_6)\sigma_{T_6}$ and δN_7 and δN_6 are the concentration changes of ^{7}Li and ^{6}Li in the breeding zones due to burnup. The perturbed system, denoted by the transport operator L, accounting for burnup can be written as $L = L_o + \delta L$ where δL is the perturbation due to concentration changes of ^{6}Li and ^{7}Li (or ^{6}Li, ^{7}Li and Be) caused by burnup. L_o is the transport operator at beginning of life. We will use ϕ_o and $\phi_o^\dagger$ as trial functions. Using $(\phi_o^\dagger, S) = (\Sigma_o, \phi_o)$, the ordinary Roussopoulos function, Eqn. (3), becomes

$$I_R(\phi_o^\dagger, \phi_o; \alpha) = (\phi_o^\dagger, S)\left\{1 + \frac{(\delta\Sigma, \phi_o)}{(\phi_o^\dagger, S)} - \frac{(\phi_o^\dagger, \delta L\phi_o)}{(\phi_o^\dagger, S)}\right\} \tag{20}$$

In the above expression, $(\delta\Sigma, \phi_o)/(\phi_o^\dagger, S)$ is the fractional change in the tritium breeding ratio due to concentration changes in ^{6}Li and ^{7}Li. This is just the estimate from zero-th order perturbation theory. The third term, $-(\phi_o^\dagger, \delta L\phi_o)/(\phi_o^\dagger, S)$, is the change in the breeding ratio due to the flux change induced by the lithium burnup. The results are summarized in Tables 13 and 14 for UWMAK-I and UWMAK-II, respectively. From these tables we see that burnup of ^{6}Li for one year has two effects. The decrease in the ^{6}Li concentration causes a small decrease in the tritium breeding ratio in both designs (column 1). The other is that the change in the tritium breeding ratio caused by the flux change is positive for both designs (column 2). However, the net effect is slightly negative (-0.13%) for the UWMAK-I blanket design, and slightly positive (+ 0.52%) for the UWMAK-II design. The sum of all effects gives a similar result.

IV. Conclusions

The method of variational interpolation is particularly useful as a design tool to study the effects of various blanket design choices on CTR blanket performance. This is especially true when the changes in design can be

represented as linear variations in the transport operator since no adjoint calculations are required while any number of response functions can be studied. For liquid lithium cooled blankets, the tritium breeding ratio is well above one for all structural materials of interest when there is about 5% structure in the breeding zone. A vanadium structured blanket produces the highest breeding ratio while a molybdenum structured system generates the most nuclear heating. The total nuclear heating is relatively insensitive to the percentage structure while the breeding ratio monotonically decreases as the structure content increases. For such liquid lithium blankets, natural lithium yields values of both breeding ratio and total nuclear heating that are near optimum. There is little incentive to enrich in ^{6}Li.

For solid breeder blankets using lithium aluminate, enrichment to about 90% ^{6}Li and the use of a neutron multiplier like beryllium appear essential. There is a broad optimum in the thickness of the neutron multiplying zone at between 15 and 24 cm for a blanket with stainless steel structure. Increasing the beryllium zone thickness beyond 25 cm will result in a decreased breeding ratio because of excessive neutron capture by the additional structure. The use of a low absorption structure like vanadium or aluminum would mean the breeding ratio would tend to saturate and would not show a decrease until very large beryllium zone thicknesses were used.

The effects of lithium burnup were found to be small for both liquid lithium cooled and solid breeder blankets. This is primarily related to the low burnup rate and to the insensitivity of results to small changes in the ^{6}Li to ^{7}Li ratio.

Acknowledgement

This research was supported by a grant from the Energy Research and Development Administration.

Figure Captions

Fig. 1 Schematic of the University of Wisconsin CTR blanket, UWMAK-I.

Fig. 2 The percent errors for the estimates of T_6, T_7 and tritium breeding ratio by the Schwinger variational functional, Eqn. (4), and two-point variational interpolation functional (fractional form), Eqn. (12) (UWMAK-I blanket).

Fig. 3 The tritium breeding ratio as a function of the percent stainless steel structure in the breeding zones of the UWMAK-I blanket.

Fig. 4 The spatial distribution of the tritium production rate in the UWMAK-I blanket for various enrichment of lithium in ^6Li.

Fig. 5 The tritium breeding ratio as a function of enrichment of lithium in ^6Li in the breeding zones of the UWMAK-I blanket.

Fig. 6 The total nuclear heating as a function of the percent stainless steel structure in the breeding zones of the UWMAK-I blanket.

Fig. 7 The total nuclear heating as a function of the percent ^6Li in total lithium in the UWMAK-I blanket.

Fig. 8 Equi-tritium breeding ratio contours for the UWMAK-I blanket with stainless steel structure.

Fig. 9 (A) The tritium breeding ratio as a function of the percent structure in the breeding zones for UWMAK-I type blankets with various structural materials.

(B) The total nuclear heating as a function of the percent structure in the breeding zones for UWMAK-I type blankets with various structural materials.

Fig. 10 (A) The tritium breeding ratio as a function of the percent ^6Li in total lithium for UWMAK-I type blankets with various structural materials.

(B) The total nuclear heating as a function of the percent ^6Li in total lithium for UWMAK-I type blankets with various structural materials.

Fig. 11 Equi-tritium breeding ratio contours for the blanket with niobium structure (UWMAK-I type).

Fig. 12 Equi-tritium breeding ratio contours for the blanket with molybdenum structure (UWMAK-I type).

Fig. 13 Equi-tritium breeding ratio contours for the blanket with vanadium structure (UWMAK-I type).

Fig. 14 Equi-tritium breeding ratio contours for the blanket with aluminum structure (UWMAK-I type).

Fig. 15 Equi-tritium breeding ratio contours for the standard UWMAK-I blanket with the 15 cm stainless steel reflector replaced by a 30 cm graphite reflector.

Fig. 16 Schematic of the University of Wisconsin CTR blanket, UWMAK-II.

Fig. 17 The tritium breeding ratio, total nuclear heating and Be(n,2n) reaction rate as a function of the (net) first wall thickness (UWMAK-II).

Fig. 18 The spatial distribution of the tritium production rate (^{6}Li(n,α)T) and Be(n,2n) reaction rate in the UWMAK-II blanket for 9, 18 and 27 cm beryllium zone thicknesses.

Fig. 19 The tritium breeding ratio as a function of the beryllium zone (zone 5) thickness (UWMAK-II).

Fig. 20 Equi-tritium breeding ratio contours for the UWMAK-II blanket as a function of the beryllium zone thickness and the (net) volume percent stainless steel structure in the breeding and beryllium zones.

References

1. G. C. Pomraning, J. Soc. Ind. Appl. Math., 13, 511 (1965)

2. S. Kaplan, "Synthesis Methods in Reactor Analysis," in Advances in Nuclear Science and Technology, edited by P. Greebler and E. Henly (Academic, New York, 1966) Vol. 3

3. W. M. Stacey, Jr., Variational Methods in Nuclear Reactor Physics, (Academic Press, New York and London, 1974)

4. R. W. Conn and W. M. Stacey, Jr., Nuclear Fusion, 13, 185 (1973)

5. D. E. Bartine, R. G. Alsmiller, Jr., E. M. Oblow, and F. R. Mynatt, Nucl. Sci. Eng., 55, 147 (1974)

6. E. T. Cheng and R. W. Conn, J. Math. Phys., 17, 683 (1976)

7. B. Badger et al., "UWMAK-I, A Wisconsin Toroidal Fusion Reactor Design," UWFDM-68, University of Wisconsin, Nuclear Engineering Department (1973)

8. B. Badger et al., "UWMAK-II, A Conceptual Tokamak Power Reactor Design," UWFDM-112, University of Wisconsin, Nuclear Engineering Department (1975)

9. W. W. Engle, Jr., "A User's Manual for ANISN," K-1643, Oak Ridge Gaseous Diffusion Plant (1967)

10. D. E. Bartine, F. R. Mynatt, and E. M. Oblow, "SWANLAKE, A Computer Code Utilizing ANISN Radiation Transport Calculations for Cross Section Sensitivity Analysis," ORNL-TM-3809, Oak Ridge National Laboratory (1973)

11. M. A. Abdou, L. J. Wittenberg, and C. W. Maynard, Nucl. Technol., 26, 400 (1975)

Table 1 Variational and Exact Tritium Breeding as a Function of Percent Structure in Breeding Zones in a UWMAK-I Fusion Reactor Blanket

Volume Percent Structure in Breeding Zones	Schwinger Principle				Variational Interpolation		Synthesis		(S_4P_3 - ANISN)	
	Reference ϕ and $\phi^\dagger$ at 5% Structure		Reference ϕ and $\phi^\dagger$ at 25% Structure		Reference ϕ at 5%, $\phi^\dagger$ at 25% Structure		Reference at 5% and 25% Structure			
	T_6	T_7	T_6	T_7	T_6	T_7	T_6	T_7	T_6	T_7
0%	0.863	0.725	0.881	0.808	0.866	0.740	0.862	0.720		
1%	0.863	0.691	0.880	0.761	0.865	0.702	0.862	0.689	0.862	0.689
5%	0.861	0.579	0.874	0.613	0.861	0.579	0.861	0.579	0.861	0.579
10%	0.859	0.473	0.866	0.483	0.856	0.466	0.859	0.471	0.859	0.471
15%	0.857	0.392	0.857	0.391	0.850	0.383	0.854	0.387	0.854	0.387
20%	0.855	0.329	0.847	0.322	0.843	0.319	0.846	0.321	0.846	0.321
25%	0.852	0.279	0.836	0.268	0.836	0.268	0.836	0.268	0.836	0.268
30%	0.850	0.237	0.824	0.225	0.828	0.227	0.823	0.225	0.823	0.225
35%	0.846	0.202	0.811	0.190	0.819	0.193	0.807	0.189	0.807	0.189

Table 2 Tritium Production from the $^{6}Li(n,\alpha)$ and $^{7}Li(n,n'\alpha)$ Reactions, Total Breeding Ratio and Total Nuclear Heating for UWMAK-I Type Fusion Reactor Blanket Designs with Different Percent Structural Material and Percent ^{6}Li in Total Lithium in the Breeding Zones by a Two-Point Interpolation Method

Percent Stainless Steel in Breeding Zones	5			10	15		25	
Percent ^{6}Li in Total Lithium	7.42[a]	20.0	30.0	7.42	7.42	20.0	7.42	30.0
T_6	0.861 (c)	0.946 (+0.85%)	0.965	0.856 (-0.35%)	0.850 (-0.47%)	0.947 (+0.35%)	0.836 (c)	0.974 (c)
T_7	0.579 (c)	0.495 (-0.40%)	0.429 (c)	0.466 (-1.06%)	0.383 (-1.03%)	0.329 (-1.50%)	0.268 (c)	0.201 (c)
Total Tritium Breeding Ratio	1.440 (c)	1.441 (+0.42%)	1.394 (c)	1.322 (-0.53%)	1.233 (-0.64%)	1.276 (-0.16%)	1.104 (c)	1.175 (c)
Total Nuclear Heating[b]	15.81 (c)	16.14 (+1.89%)	15.96 (c)	15.94 (-0.70%)	16.11 (+0.19%)	16.18 (+0.82%)	16.25 (c)	16.17 (c)

[a] natural lithium

[b] in units of MeV per 14.1 MeV D-T neutron

[c] reference values taken in the interpolation

Table 3 Tritium Breeding Ratio and Total Nuclear Heating in UWMAK-I Blanket; Stainless Steel

Percent Structure in Breeding Zones	Percent ^{6}Li in Total Lithium	T_6[a]	T_7[a]	Tritium[a] Breeding Ratio	Total[b] Nuclear Heating
5	7.42[c]	0.861	0.579	1.440	15.81
	30.0	0.965	0.429	1.394	15.96
25	7.42[c]	0.836	0.268	1.104	16.25
	30.0	0.974	0.201	1.175	16.17

a. in units of tritons per D-T neutron

b. in units of MeV per 14.1 MeV D-T neutron

c. natural lithium

Table 4 Tritium Breeding Ratio and Total Nuclear Heating in UWMAK-I Blanket; Niobium Structure

Percent Structure in Breeding Zones	Percent ^{6}Li in Total Lithium	T_6[a]	T_7[a]	Tritium[a] Breeding Ratio	Total[b] Nuclear Heating
5	7.42[c]	0.724	0.576	1.300	16.58
	30.0	1.028	0.427	1.455	16.32
25	7.42[c]	0.573	0.267	0.840	18.01
	30.0	1.062	0.198	1.260	17.15

a. in units of tritons per D-T neutron

b. in units of MeV per 14.1 MeV D-T neutron

c. natural lithium

Table 5 Tritium Breeding Ratio and Total Nuclear Heating in UWMAK-I Blanket; Molybdenum Structure

Percent Structure in Breeding Zones	Percent ^{6}Li in Total Lithium	T_6[a]	T_7[a]	Tritium[a] Breeding Ratio	Total[b] Nuclear Heating
5	7.42[c]	0.819	0.588	1.407	16.61
	30.0	1.100	0.437	1.537	16.58
25	7.42[c]	0.685	0.286	0.971	18.94
	30.0	1.198	0.215	1.413	17.77

a. in units of tritons per D-T neutron

b. in units of MeV per 14.1 MeV D-T neutron

c. natural lithium

Table 6 Tritium Breeding Ratio and Total Nuclear Heating in UWMAK-I Blanket; Vanadium Structure

Percent Structure in Breeding Zones	Percent ^{6}Li in Total Lithium	T_6[a]	T_7[a]	Tritium[a] Breeding Ratio	Total[b] Nuclear Heating
5	7.42[c]	0.960	0.637	1.597	15.59
	30.0	1.062	0.471	1.533	15.80
25	7.42[c]	1.053	0.340	1.393	15.99
	30.0	1.191	0.255	1.446	15.85

a. in units of tritons per D-T neutron

b. in units of MeV per 14.1 MeV D-T neutron

c. natural lithium

Table 7 Tritium Breeding Ratio and Total Nuclear Heating in UWMAK-I Blanket; Aluminum Structure

Percent Structure in Breeding Zones	Percent ^{6}Li in Total Lithium	T_6[a]	T_7[a]	Tritium[a] Breeding Ratio	Total[b] Nuclear Heating
5	7.42[c]	0.759	0.698	1.457	14.65
	30.0	0.903	0.512	1.415	15.38
25	7.42[c]	0.690	0.433	1.123	14.68
	30.0	0.833	0.321	1.154	15.33

a. in units of tritons per D-T neutron

b. in units of MeV per 14.1 MeV D-T neutron

c. natural lithium

Table 8 Tritium Breeding Ratio and Total Nuclear Heating in UWMAK-I Blanket; Stainless Steel (replace stainless steel reflector by a 30 cm graphite reflector)

Percent Structure in Breeding Zones	Percent ^{6}Li in Total Lithium	T_6[a]	T_7[a]	Tritium[a] Breeding Ratio	Total[b] Nuclear Heating
5	7.42[c]	0.952	0.581	1.533	16.32
	30.0	1.005	0.431	1.436	15.95
25	7.42[c]	0.976	0.268	1.244	16.35
	30.0	1.001	0.201	1.202	16.22

a. in units of tritons per D-T neutron

b. in units of MeV per 14.1 MeV D-T neutron

c. natural lithium

Table 9 Comparison of Tritium Breeding Ratio[a] in UWMAK-II Blanket for Several Beryllium Zone Thicknesses

Net Percent Structure in Breeding and Beryllium Zones[b]	5			10		
Beryllium Zone Thickness, cm (Zone 5)	9	18	27	9	18	27
T_6 in Zone 4	0.3520	0.5466	0.6314	0.3607	0.5275	0.5819
T_6 in Zone 6	0.6503	0.6400	0.5196	0.6284	0.5742	0.4241
Sum of T_6	1.0023	1.1866	1.1510	0.9891	1.1017	1.0060
Be(n,T)	0.0071	0.0096	0.0107	0.0065	0.0085	0.0094
Sum of T_7	0.0043	0.0034	0.0029	0.0038	0.0030	0.0026
Tritium Breeding Ratio	1.0137	1.1996	1.1646	0.9994	1.1132	1.0180

a. in units of tritons/D-T neutron

b. the amounts of lithium aluminate and beryllium are left unchanged

Table 10 Comparison of Neutron Balance[a] in UWMAK-II Blanket for Several Beryllium Zone Thicknesses

Net Percent Structure in Breeding and Beryllium Zones[a]	5			10		
Beryllium Zone Thickness, cm (Zone 5)	9	18	27	9	18	27
Be(n,2n)	0.3695	0.5610	0.6642	0.3274	0.4814	0.5594
Non-Tritium Production Absorption	0.4007	0.4235	0.5737	0.3957	0.4535	0.6374
Neutron Leakage	0.0543	0.0488	0.0210	0.0463	0.0386	0.0221

a. in units of reaction/D-T neutron

b. the amounts of lithium aluminate and beryllium are left unchanged

Table 11 Comparison of Nuclear Heating[a] in UWMAK-II Blanket for Several Beryllium Zone Thicknesses

Net Percent Structure in Breeding and Beryllium Zones[b]	5			10		
Beryllium Zone Thickness, cm (Zone 5)	9	18	27	9	18	27
Neutron Heating	11.45	12.77	12.82	11.03	11.89	11.57
Gamma Heating	4.71	5.39	5.85	6.09	6.61	6.97
Total Nuclear Heating	16.16	18.16	18.67	17.12	18.50	18.54
Neutron Energy Leakage	0.061	0.038	0.023	0.051	0.029	0.016

a. in units of MeV/14.1 MeV neutron

b. the amounts of lithium aluminate and beryllium are left unchanged

Table 12

Important Nuclide Burn-up Rates in
Fusion Reactor Blankets (%)*

Nuclide	UWMAK-I	UWMAK-II
^{6}Li	0.67%	1.29%
^{7}Li	0.036%	0.03%
Be	-	0.09%

*based on $1MW/m^2$ neutron wall loading, continous operation for one year

Table 13

Sensitivity of Tritium Breeding to Burn-up of Li in UWMAK-I (in %/MW/m^2 of Wall Loading) - Natural Lithium and One Year of Burn-up

Type of Perturbation and Response	1 $\frac{(\delta\Sigma,\phi)}{(\phi^+,S)}$	2 $-\frac{(\phi^+,\delta L\phi)}{(\phi^+,S)}$	3 Net Effect
Burn-up of ^{6}Li on T Production from ^{6}Li	-0.470	+0.342	-0.128
Burn-up of ^{6}Li on T Production from ^{7}Li	0	+0.014	0.014
Burn-up of ^{7}Li on T Production from ^{6}Li	0	-0.004	-0.004
Burn-up of ^{7}Li on T Production from ^{7}Li	-0.025	+0.008	-0.017
TOTAL of Above Effects	-0.495%	+0.360%	-0.135%

Table 14

Sensitivity of Tritium Breeding to Burn-up of Li and Be in UWMAK-II (in %/MW/m^2 of Wall Loading)

Lithium Enriched to 90% Li-6 and One Year of Burn Up

Type of Perturbation and Response	1 $\frac{(\delta\Sigma,\phi)}{(\phi^+,S)}$	2 $-\frac{(\phi^+,\delta L\phi)}{(\phi^+,S)}$	3 Net Effect*
Burn-up of ^{6}Li on T Production from ^{6}Li	-1.95	+2.47	+0.52
Burn-up of ^{6}Li on T Production from ^{7}Li	0	negligible	negligible
Burn-up of ^{7}Li on T Production from ^{6}Li and ^{7}Li	negligible	negligible	negligible
Burn-up of ^{9}Be on T Production from ^{6}Li	0	-0.02	-0.02
TOTAL of Above Effects	-1.95%	+2.45%	+0.50%

*Using nonuniform burn-up.

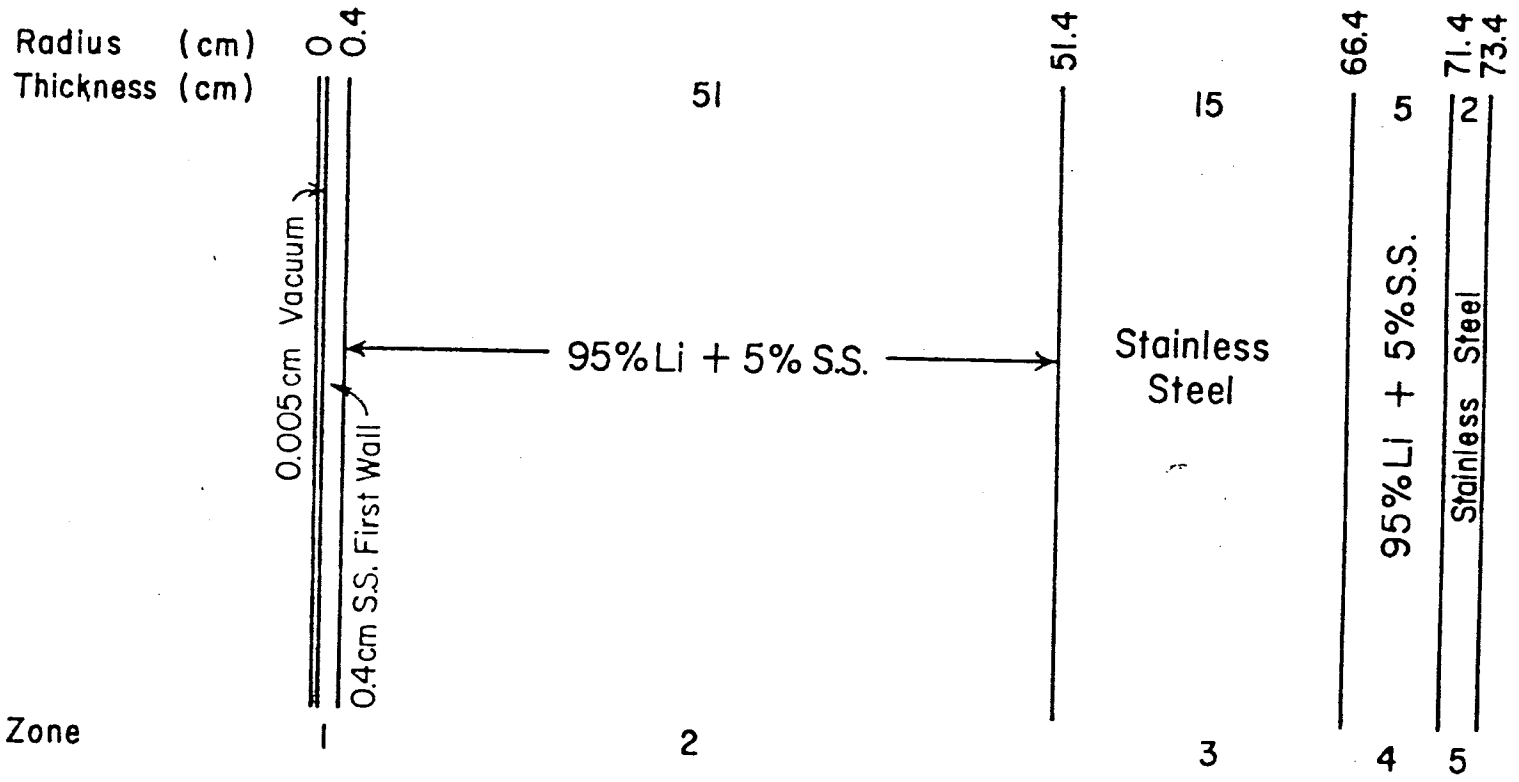

University of Wisconsin CTR Blanket Structure

UWMAK-I

Figure 1

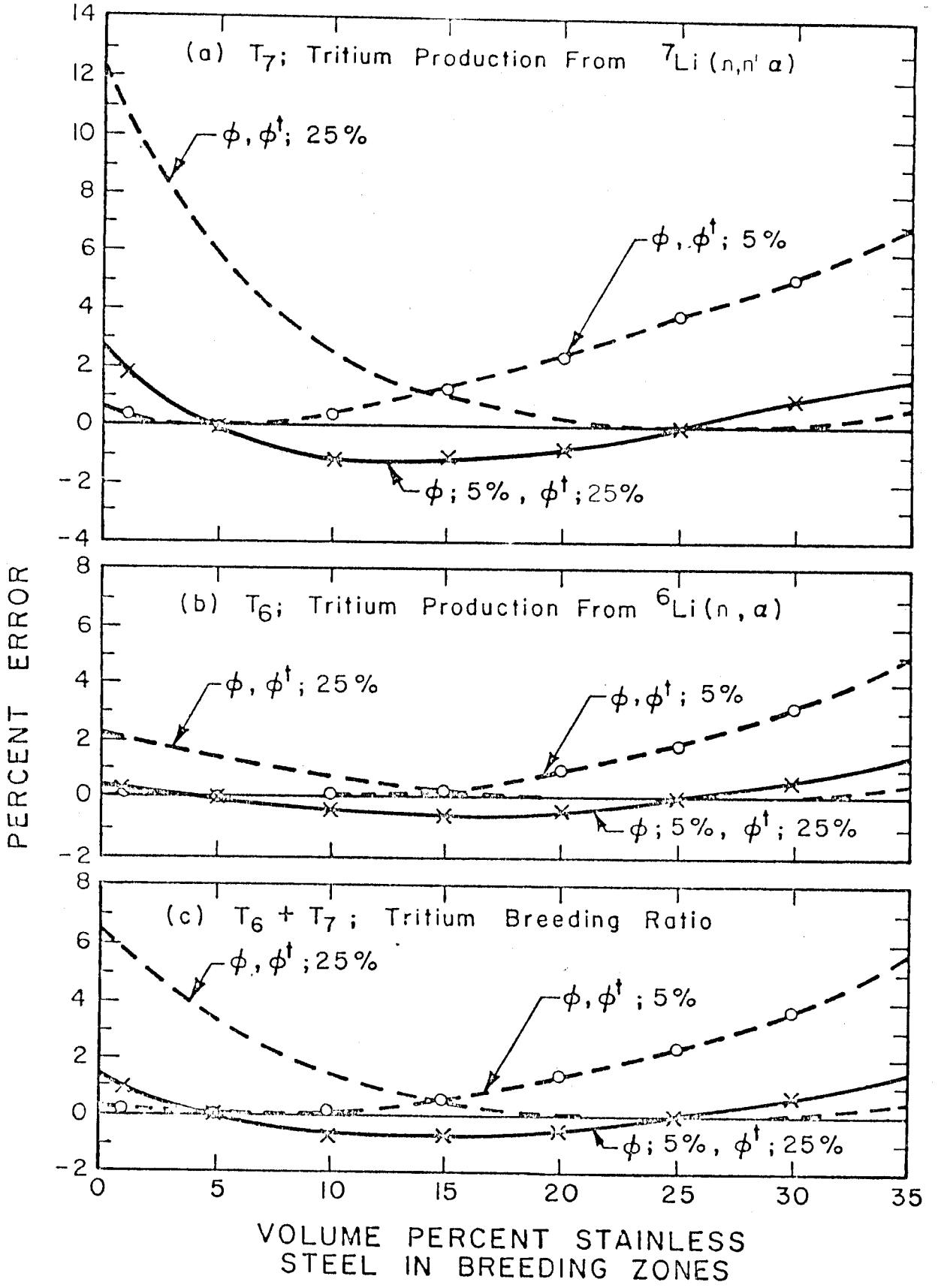
(a) T_7; Tritium Production From $^7Li(n,n'\alpha)$
ϕ, ϕ^t; 25%
ϕ, ϕ^t; 5%
ϕ; 5%, ϕ^t; 25%
(b) T_6; Tritium Production From $^6Li(n,\alpha)$
ϕ, ϕ^t; 25%
ϕ, ϕ^t; 5%
ϕ; 5%, ϕ^t; 25%
(c) $T_6 + T_7$; Tritium Breeding Ratio
ϕ, ϕ^t; 25%
ϕ, ϕ^t; 5%
ϕ; 5%, ϕ^t; 25%
PERCENT ERROR
VOLUME PERCENT STAINLESS STEEL IN BREEDING ZONES

Figure 2

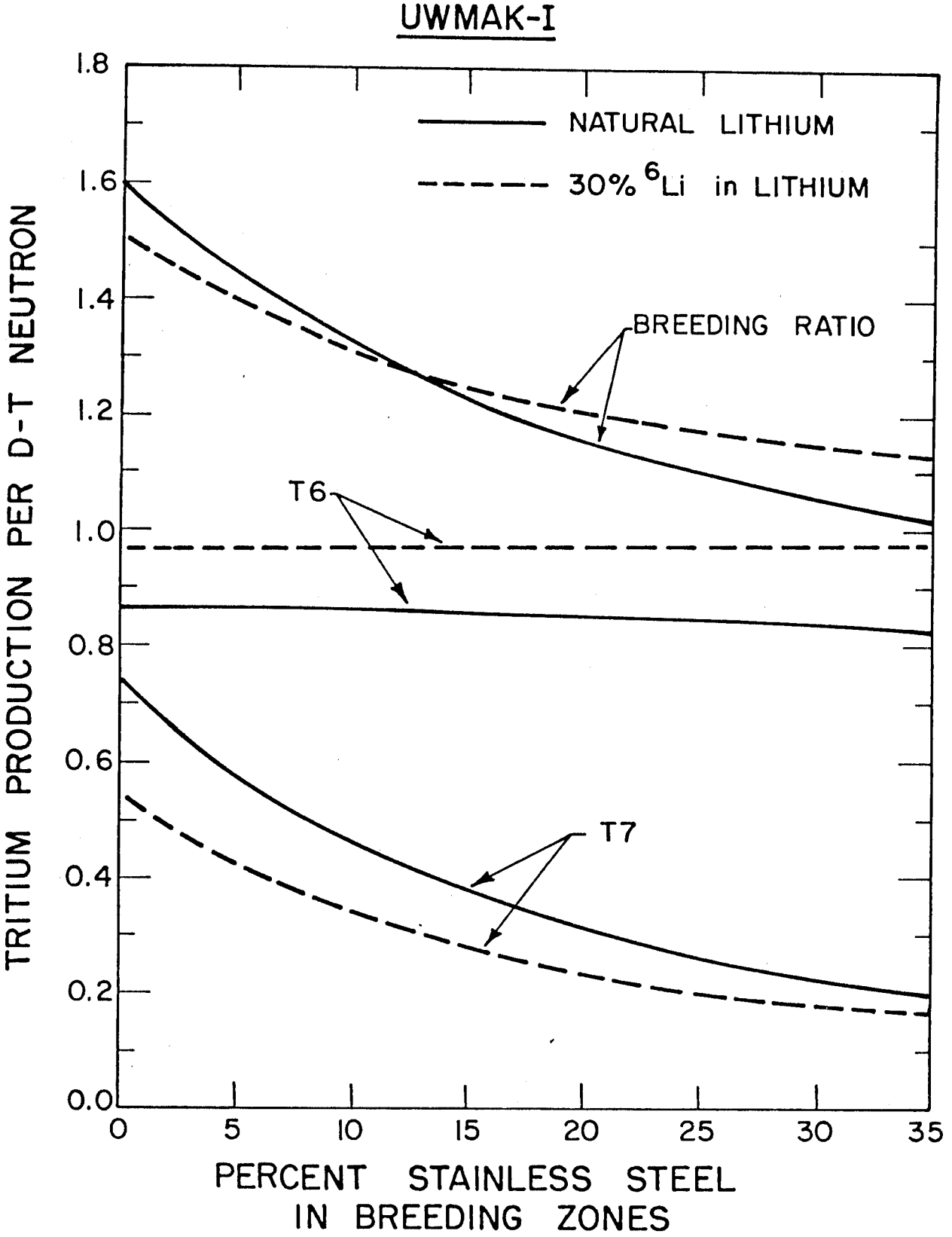
UWMAK-I
NATURAL LITHIUM
30% ^{6}Li in LITHIUM
BREEDING RATIO
T6
T7
TRITIUM PRODUCTION PER D-T NEUTRON
PERCENT STAINLESS STEEL IN BREEDING ZONES
0.0
0.2
0.4
0.6
0.8
1.0
1.2
1.4
1.6
1.8
0
5
10
15
20
25
30
35

Figure 3

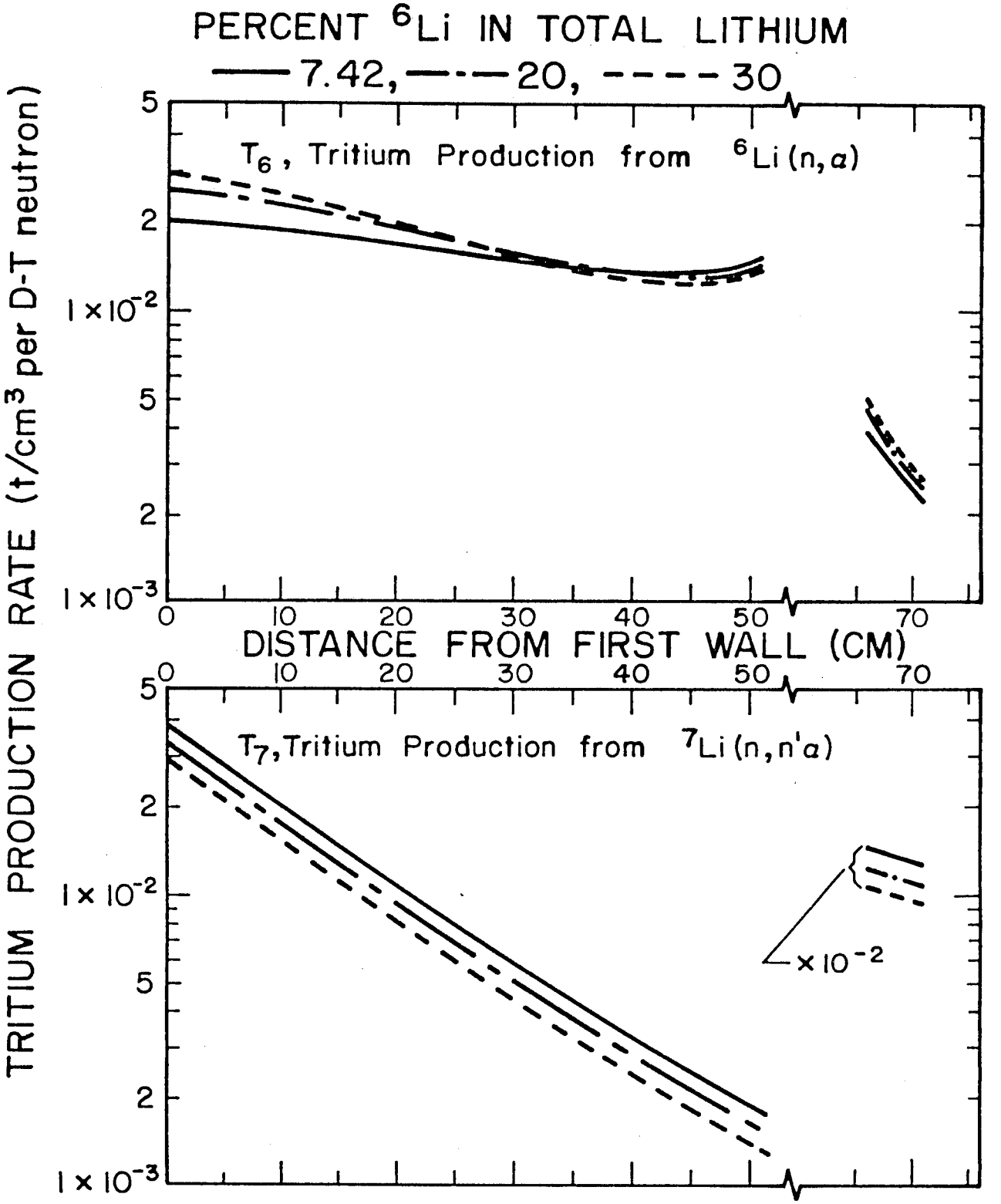
PERCENT ^{6}Li IN TOTAL LITHIUM
7.42, 20, 30
T_6, Tritium Production from ^{6}Li (n, α)
T_7, Tritium Production from ^{7}Li (n, n'α)
TRITIUM PRODUCTION RATE (t/cm^3 per D-T neutron)
DISTANCE FROM FIRST WALL (CM)
0
10
20
30
40
50
70
5
2
1 x 10^{-2}
5
2
1 x 10^{-3}
x 10^{-2}

Figure 4

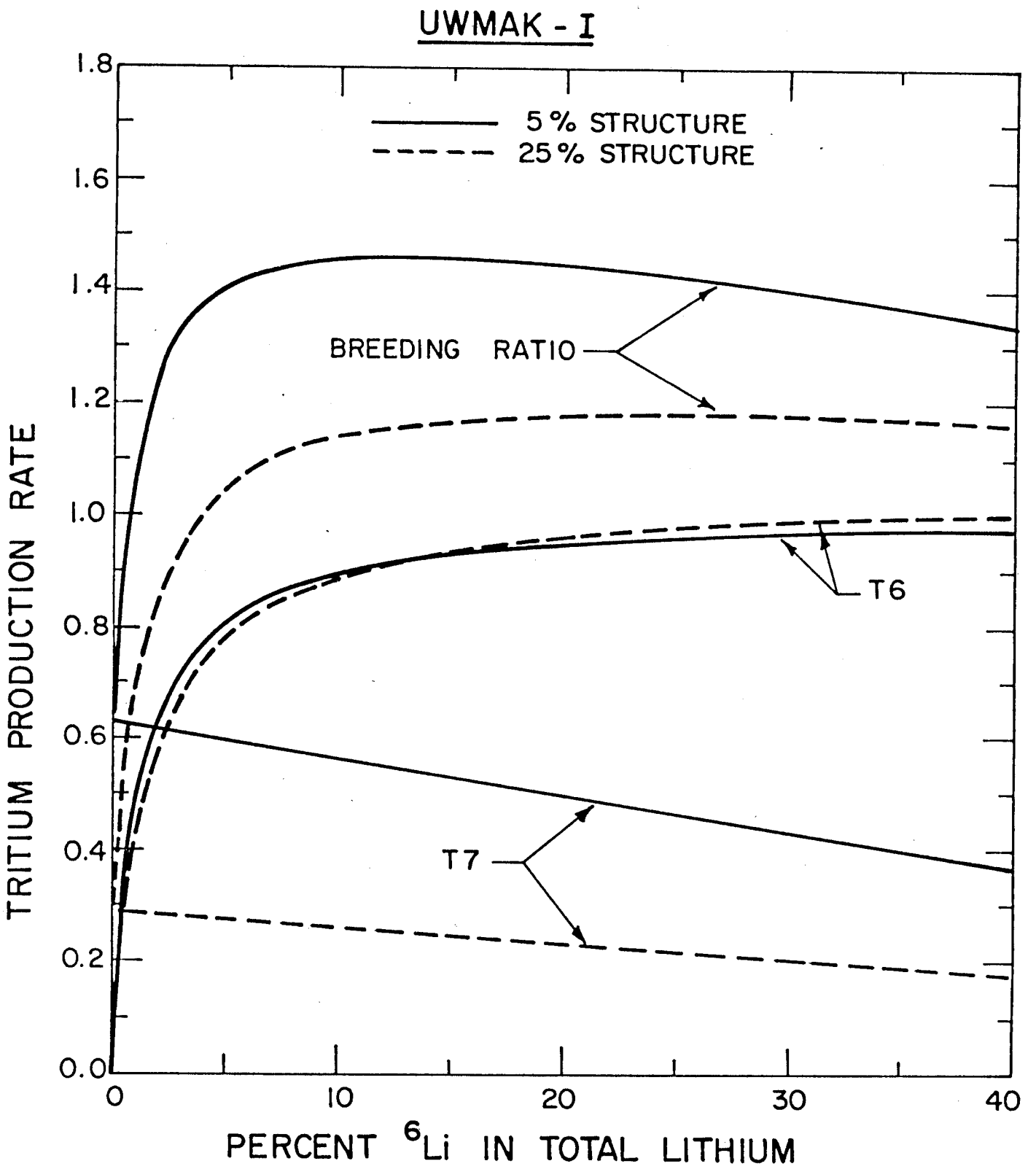
UWMAK - I
5 % STRUCTURE
25 % STRUCTURE
BREEDING RATIO
T6
T7
TRITIUM PRODUCTION RATE
PERCENT ^{6}Li IN TOTAL LITHIUM
0.0
0.2
0.4
0.6
0.8
1.0
1.2
1.4
1.6
1.8
0
10
20
30
40

Figure 5

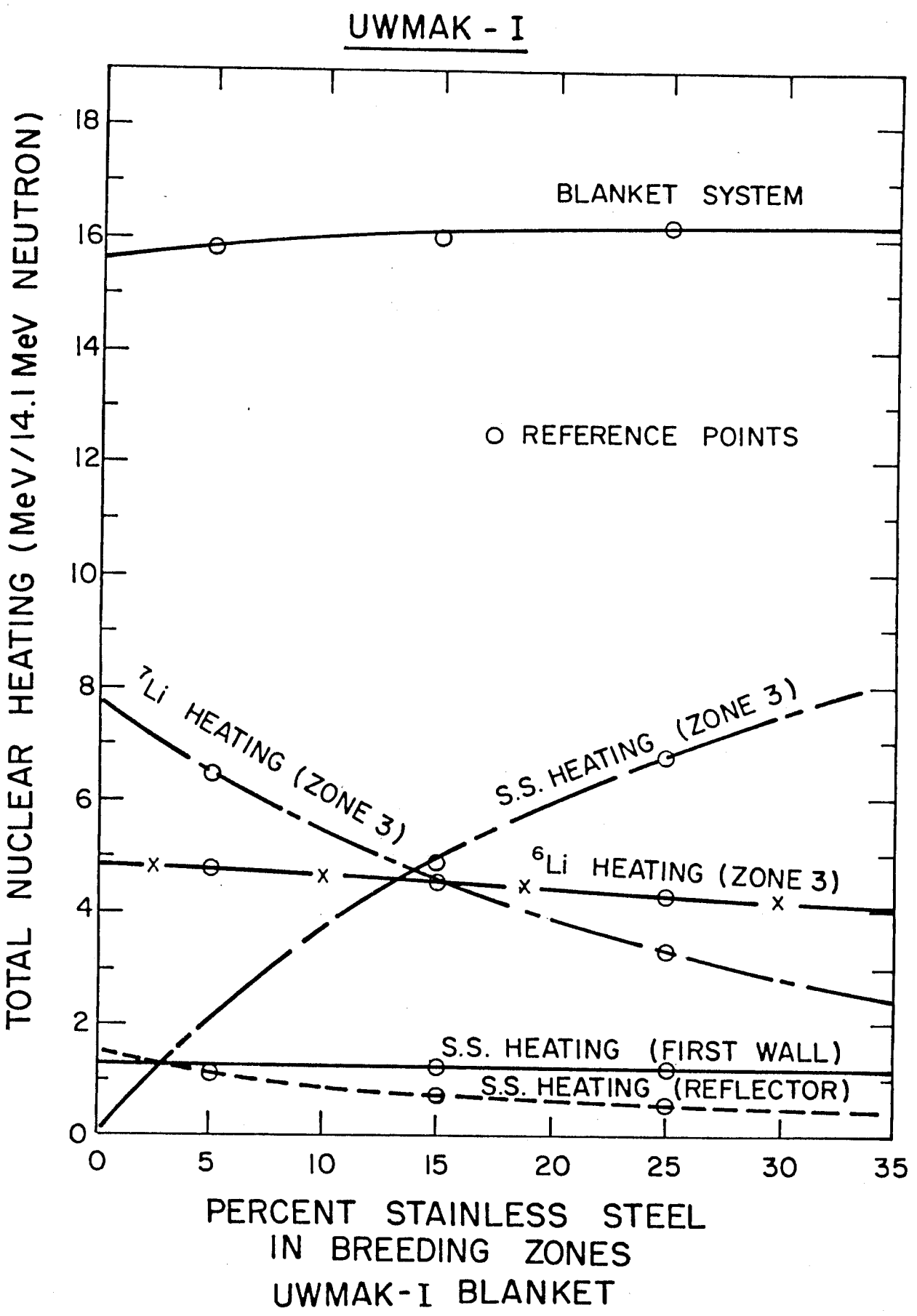
UWMAK - I
TOTAL NUCLEAR HEATING (MeV/14.1 MeV NEUTRON)
BLANKET SYSTEM
O REFERENCE POINTS
^{7}Li HEATING (ZONE 3)
S.S. HEATING (ZONE 3)
^{6}Li HEATING (ZONE 3)
S.S. HEATING (FIRST WALL)
S.S. HEATING (REFLECTOR)
PERCENT STAINLESS STEEL
IN BREEDING ZONES
UWMAK-I BLANKET

Figure 6

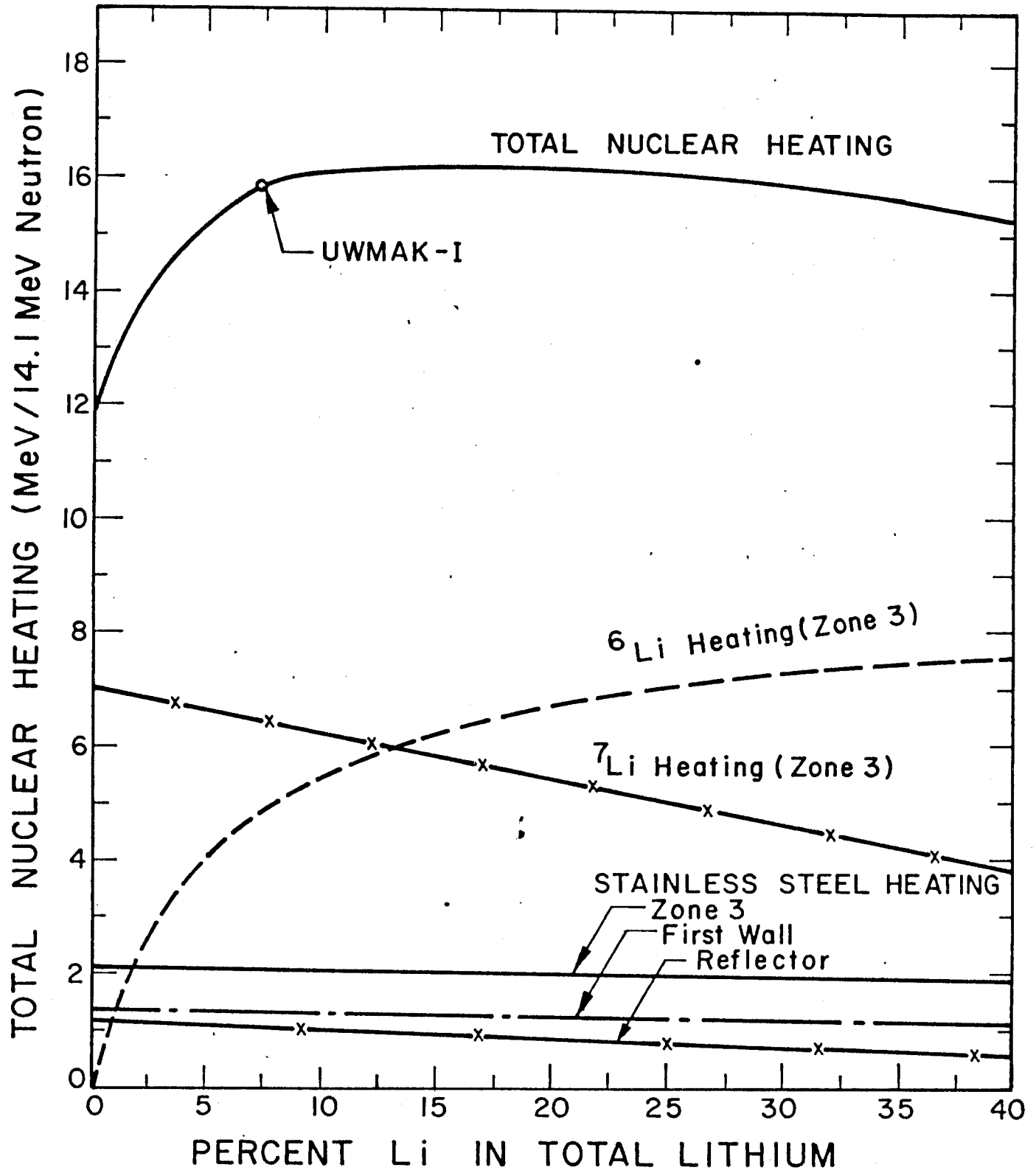
TOTAL NUCLEAR HEATING (MeV/14.1 MeV Neutron)
PERCENT Li IN TOTAL LITHIUM
TOTAL NUCLEAR HEATING
UWMAK-I
6Li Heating (Zone 3)
7Li Heating (Zone 3)
STAINLESS STEEL HEATING
Zone 3
First Wall
Reflector
0
2
4
6
8
10
12
14
16
18
0
5
10
15
20
25
30
35
40

Figure 7

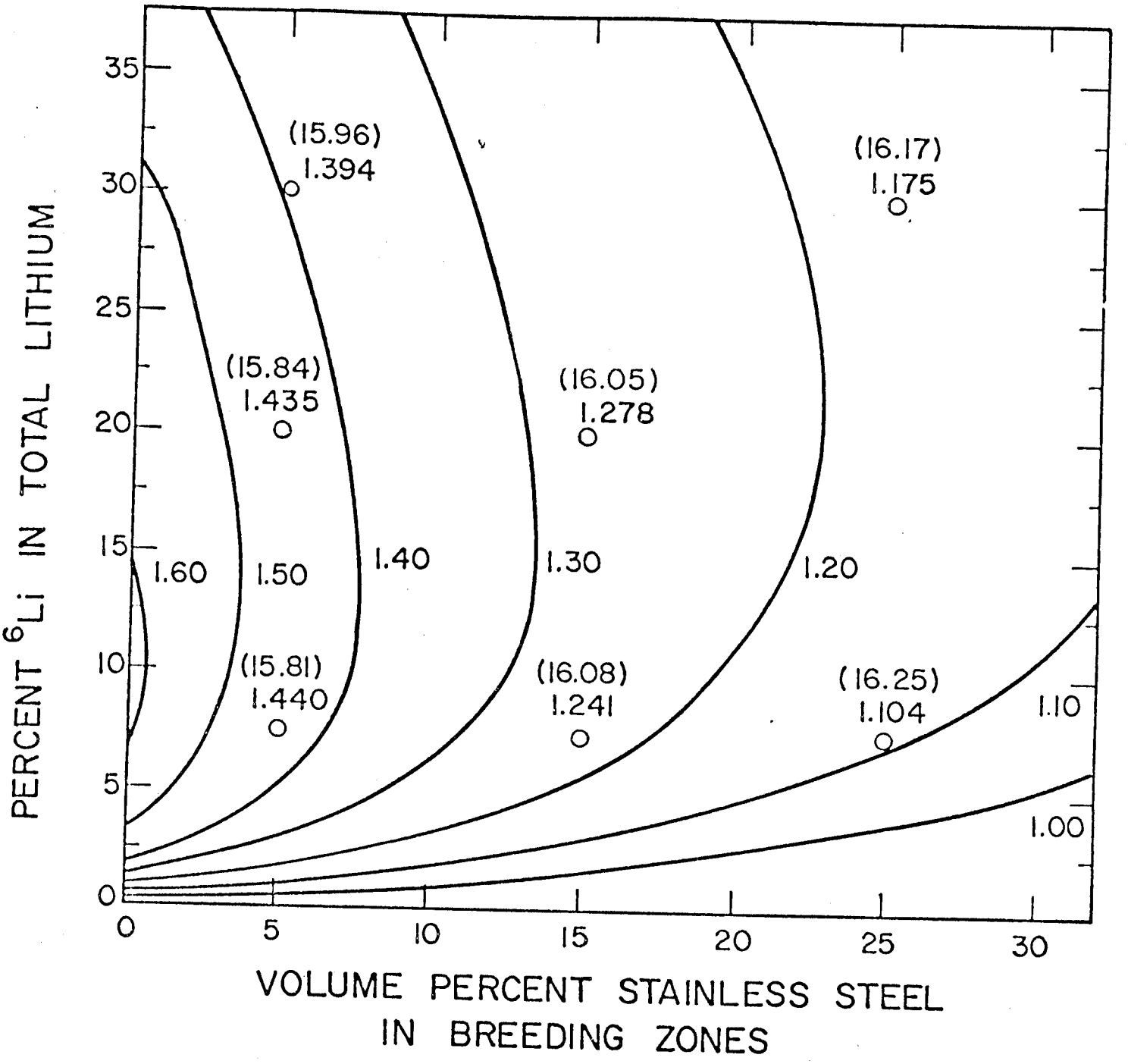

Equi-breeding ratio contours

Figure 8

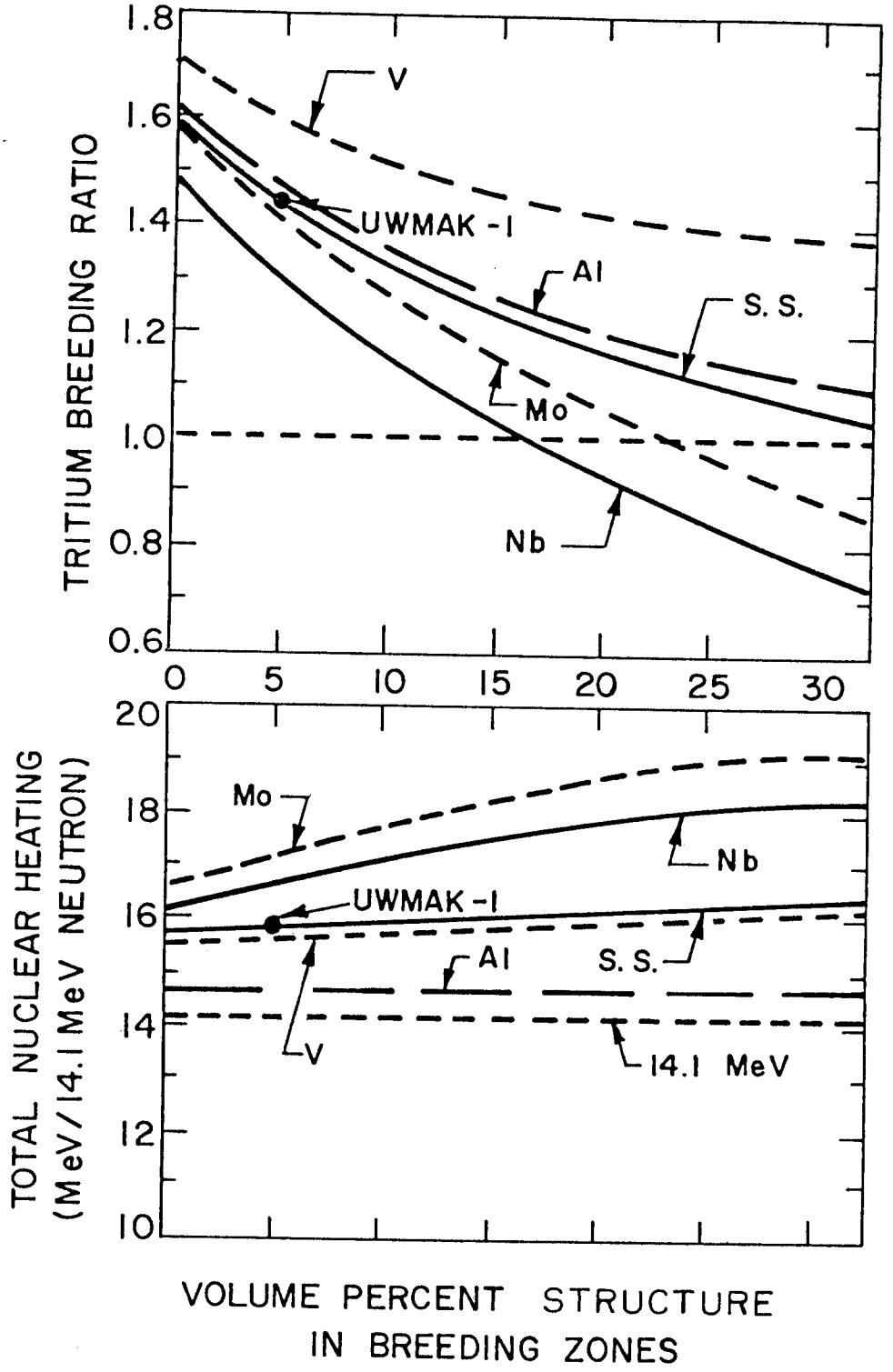
TRITIUM BREEDING RATIO
1.8
1.6
1.4
1.2
1.0
0.8
0.6
V
UWMAK-I
Al
S.S.
Mo
Nb
0
5
10
15
20
25
30
TOTAL NUCLEAR HEATING (MeV/14.1 MeV NEUTRON)
20
18
16
14
12
10
Mo
Nb
UWMAK-I
Al
S.S.
V
14.1 MeV
VOLUME PERCENT STRUCTURE IN BREEDING ZONES

Figure 9

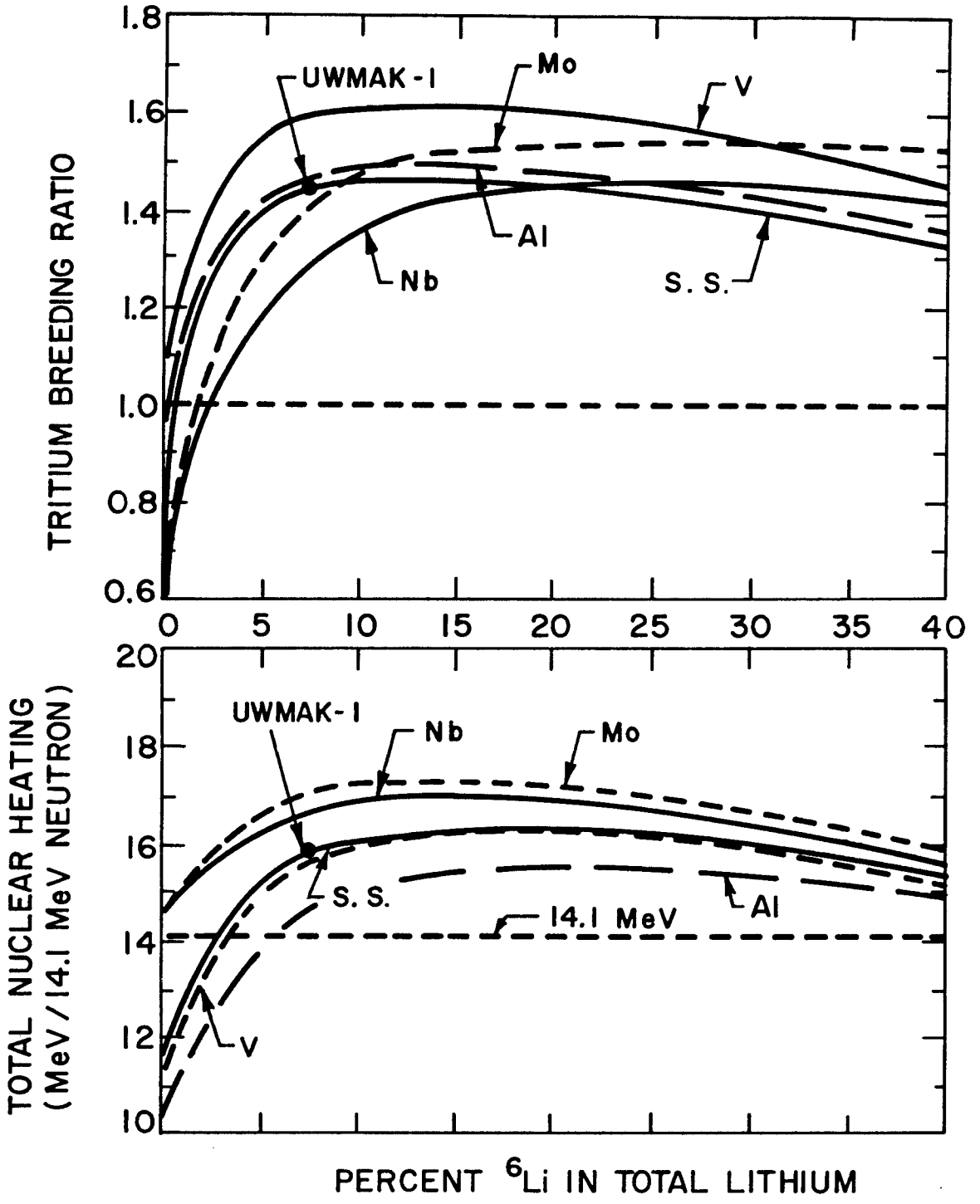
TRITIUM BREEDING RATIO
1.8
1.6
1.4
1.2
1.0
0.8
0.6
UWMAK-I
Mo
V
Al
Nb
S. S.
0
5
10
15
20
25
30
35
40
TOTAL NUCLEAR HEATING
(MeV/14.1 MeV NEUTRON)
20
18
16
14
12
10
UWMAK-I
Nb
Mo
S. S.
Al
14.1 MeV
V
PERCENT ^{6}Li IN TOTAL LITHIUM

Figure 10

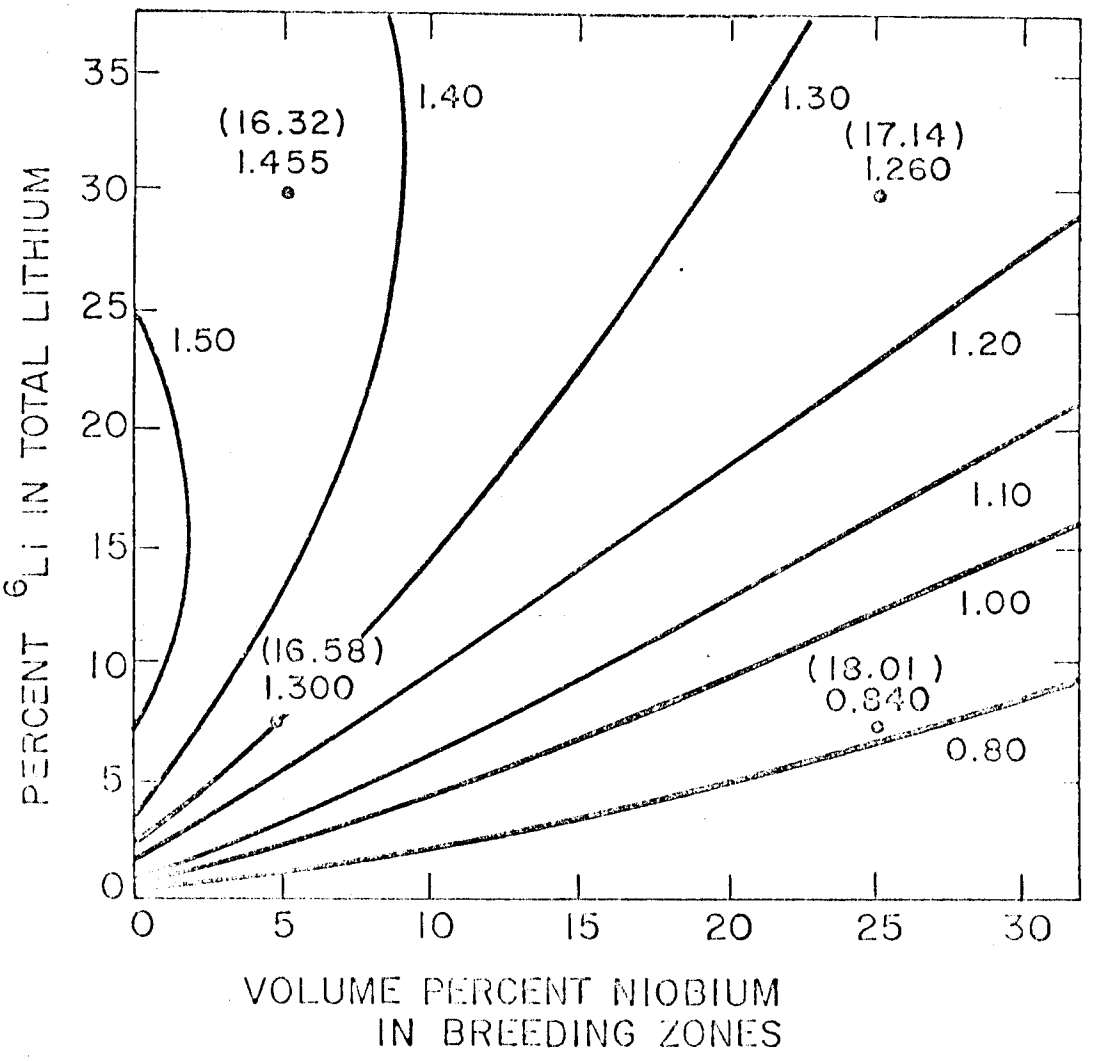
PERCENT ^{6}Li IN TOTAL LITHIUM
VOLUME PERCENT NIOBIUM IN BREEDING ZONES
0
5
10
15
20
25
30
35
(16.32)
1.455
1.40
1.30
(17.14)
1.260
1.50
1.20
1.10
1.00
(16.58)
1.300
(18.01)
0.840
0.80

Figure 11

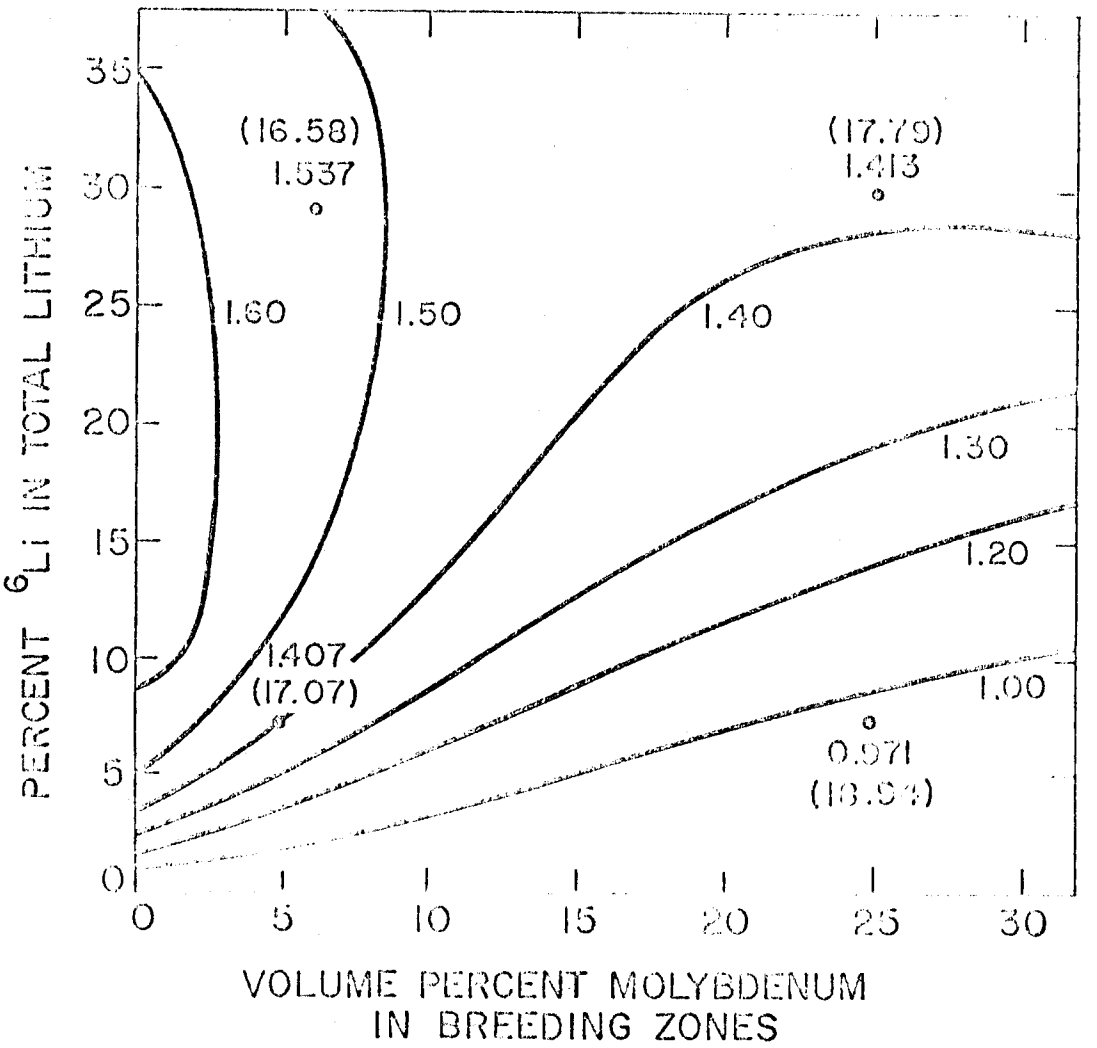
PERCENT ^{6}Li IN TOTAL LITHIUM
VOLUME PERCENT MOLYBDENUM IN BREEDING ZONES
0
5
10
15
20
25
30
35
(16.58)
1.537
(17.79)
1.413
1.60
1.50
1.40
1.30
1.20
1.00
1.407
(17.07)
0.971
(18.94)

Figure 12

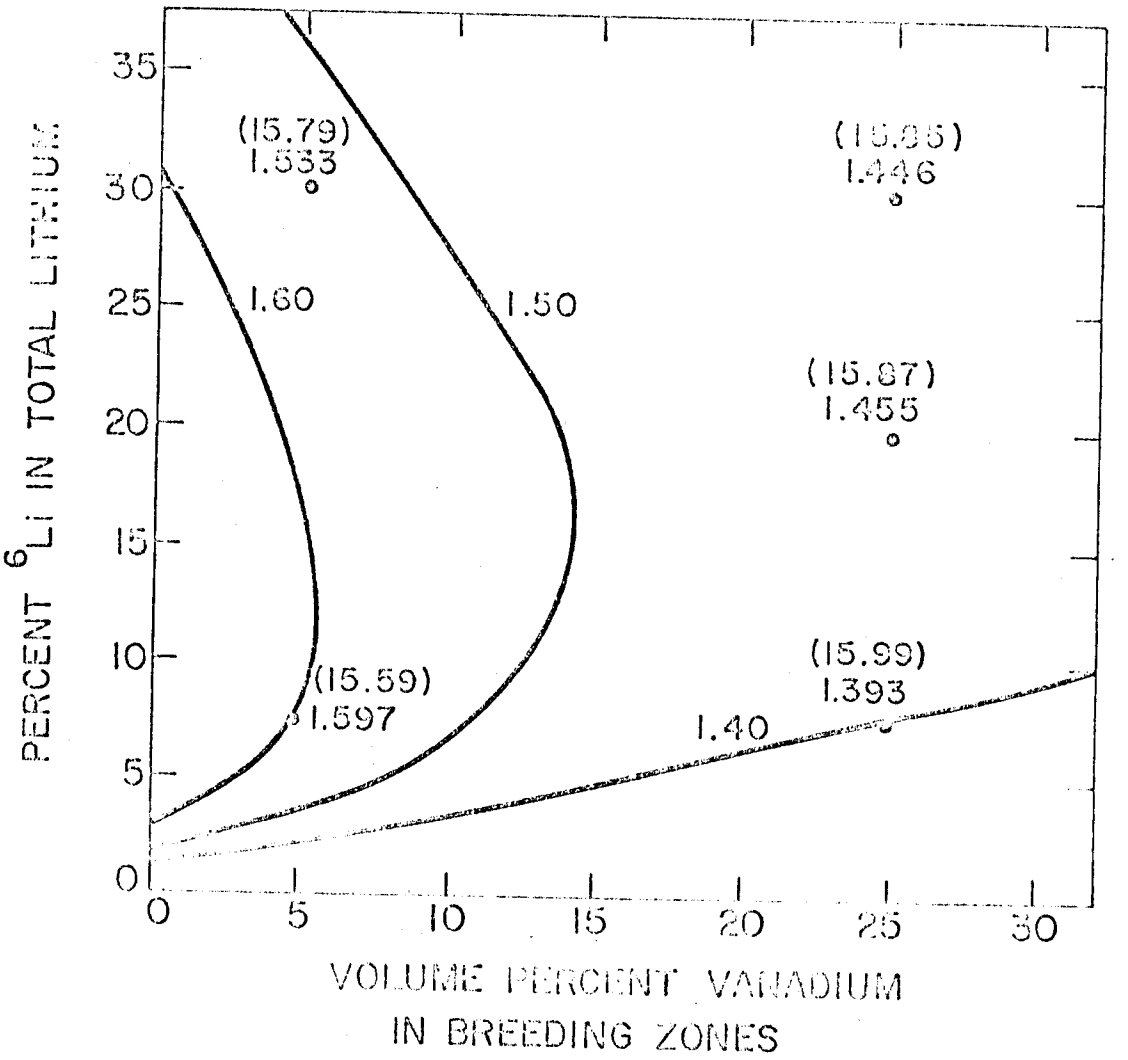
PERCENT ^{6}Li IN TOTAL LITHIUM
35
30
25
20
15
10
5
0
0
5
10
15
20
25
30
VOLUME PERCENT VANADIUM
IN BREEDING ZONES
(15.79)
1.533
(15.85)
1.446
1.60
1.50
(15.87)
1.455
(15.59)
1.597
(15.99)
1.393
1.40

Figure 13

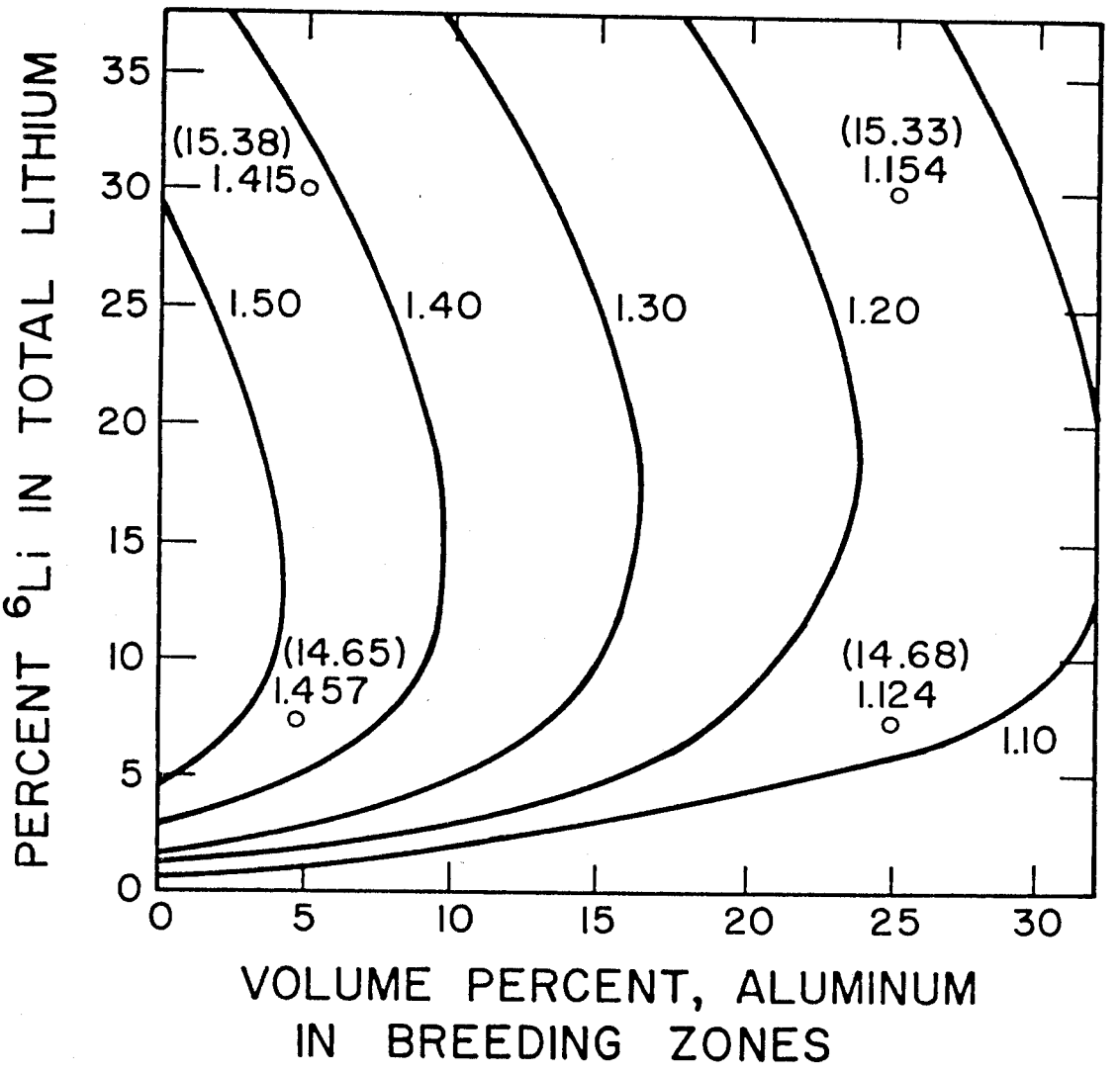
PERCENT ^{6}Li IN TOTAL LITHIUM
VOLUME PERCENT, ALUMINUM IN BREEDING ZONES
0
5
10
15
20
25
30
35
(15.38)
1.415
1.50
1.40
1.30
1.20
(15.33)
1.154
(14.65)
1.457
(14.68)
1.124
1.10

Figure 14

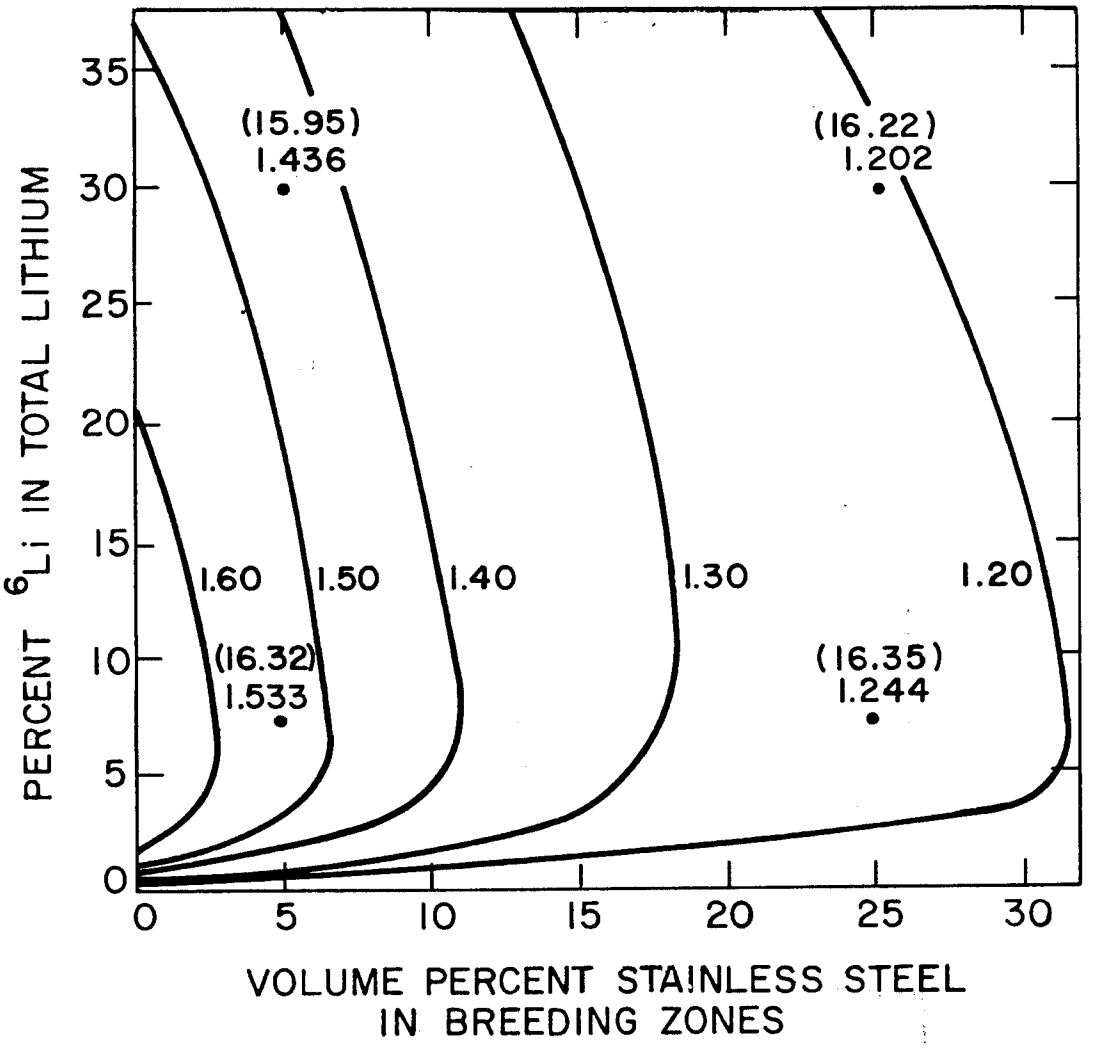
PERCENT ^{6}Li IN TOTAL LITHIUM
VOLUME PERCENT STAINLESS STEEL IN BREEDING ZONES
0
5
10
15
20
25
30
35
(15.95)
1.436
(16.22)
1.202
1.60
1.50
1.40
1.30
1.20
(16.32)
1.533
(16.35)
1.244

Figure 15

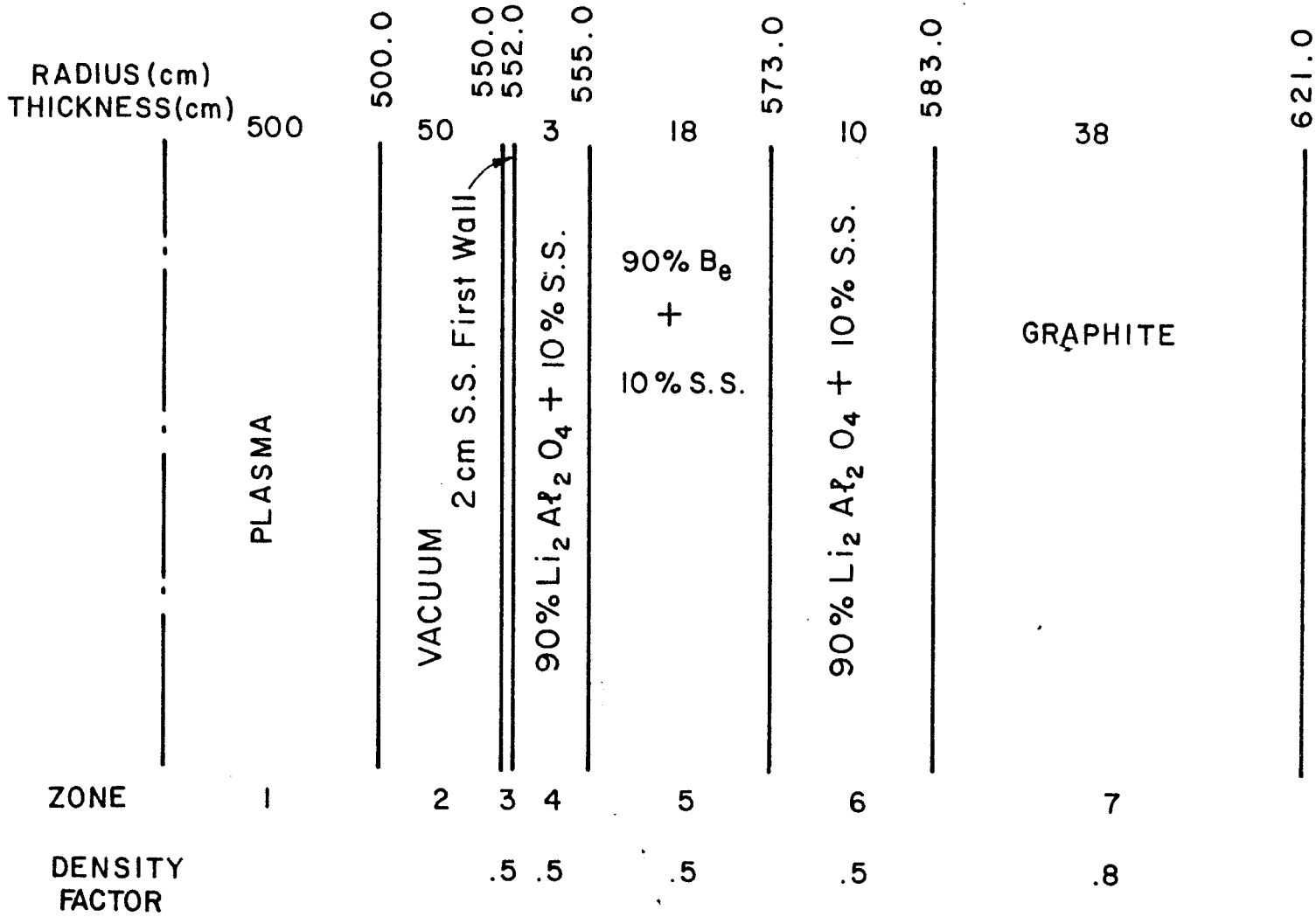

UNIVERSITY OF WISCONSIN CTR BLANKET STRUCTURE

UWMAK - II

Figure 16

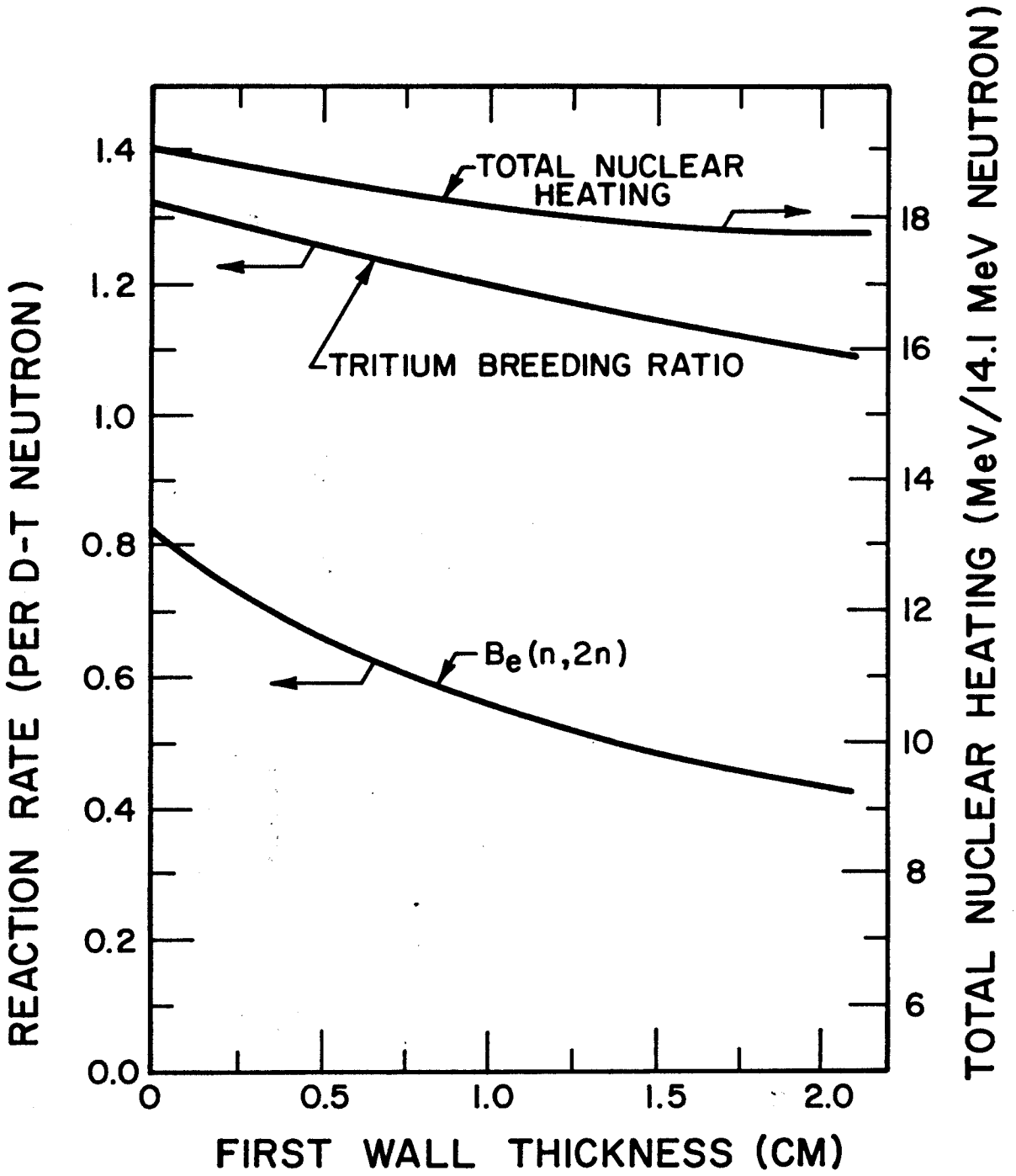
TOTAL NUCLEAR HEATING
TRITIUM BREEDING RATIO
$B_e(n,2n)$
REACTION RATE (PER D-T NEUTRON)
TOTAL NUCLEAR HEATING (MeV/14.1 MeV NEUTRON)
FIRST WALL THICKNESS (CM)
0.0
0.2
0.4
0.6
0.8
1.0
1.2
1.4
6
8
10
12
14
16
18
0
0.5
1.0
1.5
2.0

Figure 17

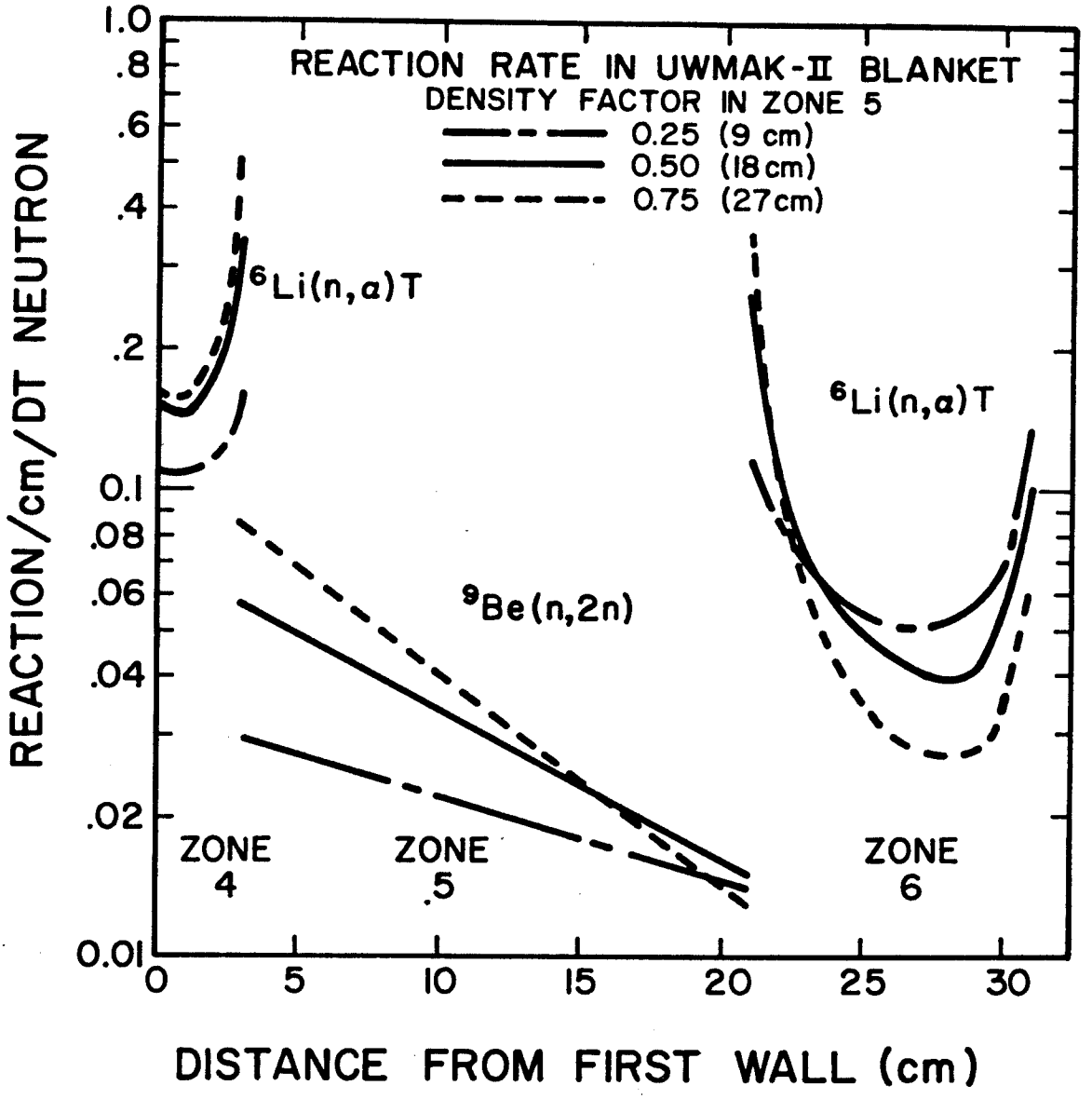
REACTION RATE IN UWMAK-II BLANKET
DENSITY FACTOR IN ZONE 5
0.25 (9 cm)
0.50 (18 cm)
0.75 (27 cm)
^{6}Li(n,α)T
^{6}Li(n,α)T
^{9}Be(n,2n)
ZONE 4
ZONE 5
ZONE 6
REACTION/cm/DT NEUTRON
DISTANCE FROM FIRST WALL (cm)
1.0
.8
.6
.4
.2
0.1
.08
.06
.04
.02
0.01
0
5
10
15
20
25
30

Figure 18

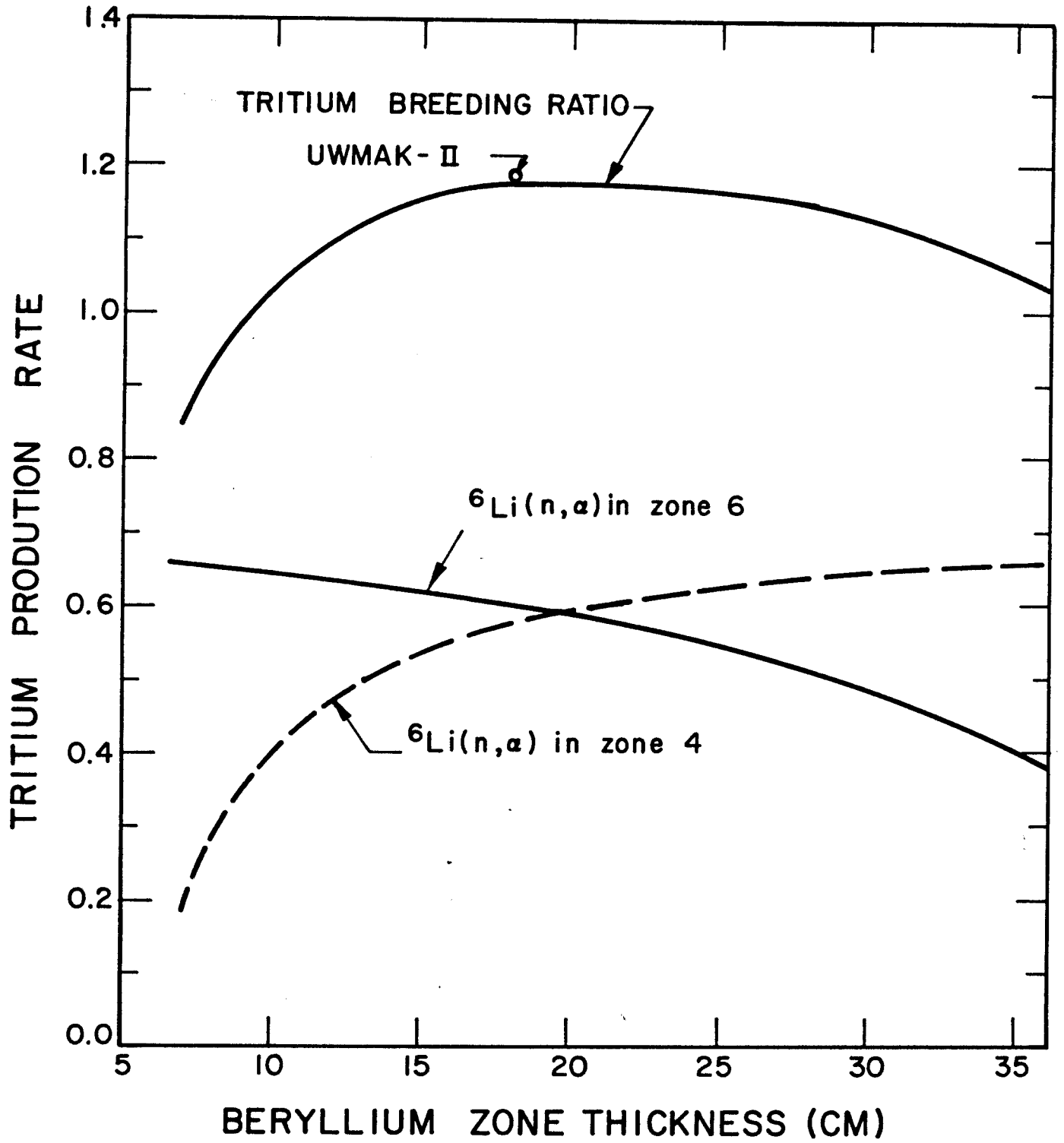
TRITIUM BREEDING RATIO
UWMAK-II
^{6}Li(n,α)in zone 6
^{6}Li(n,α) in zone 4
TRITIUM PRODUTION RATE
BERYLLIUM ZONE THICKNESS (CM)
1.4
1.2
1.0
0.8
0.6
0.4
0.2
0.0
5
10
15
20
25
30
35

Figure 19

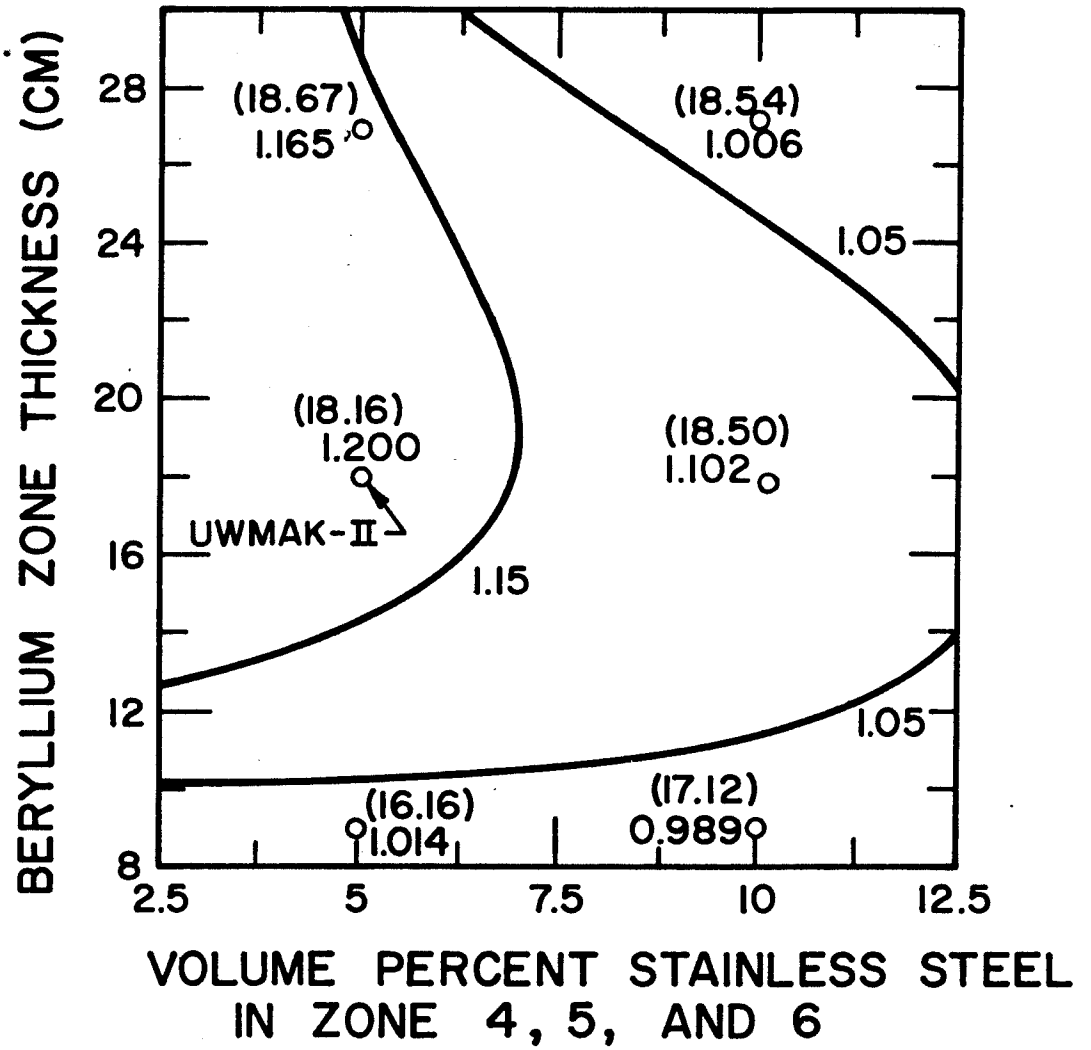
BERYLLIUM ZONE THICKNESS (CM)
28
24
20
16
12
8
2.5
5
7.5
10
12.5
(18.67)
1.165
(18.54)
1.006
1.05
(18.16)
1.200
UWMAK-II
(18.50)
1.102
1.15
1.05
(16.16)
1.014
(17.12)
0.989
VOLUME PERCENT STAINLESS STEEL
IN ZONE 4, 5, AND 6

Figure 20